VIRGO

*A primer on a **Real** Gravitational Wave Detector*

Fulvio Ricci
University of Rome La Sapienza
&
INFN Sezione di Roma

SAPIENZA
UNIVERSITÀ DI ROMA

INFN
Istituto Nazionale di Fisica Nucleare

Talk outline

Basic concepts

- *Laudatio (encomium)* of the Modulation Method
- Formalism to treat optical elements
- Michelson Interferometer
- F-P cavity
- Light detection method
- Interferometer Control
- Sensitivity
- Conclusion ➔ the Virgo detector

Introduction to modulation

- Modulation is the process by which some characteristic of the carrier is varied in accordance with a modulation wave
- It permits to put information onto a high frequency carrier for transmission (*frequency translation*)
- In the modulation process, the modulation wave is at lower frequency, "the baseband signal", while the signal transporting the information , "*the carrier*", is at higher frequency

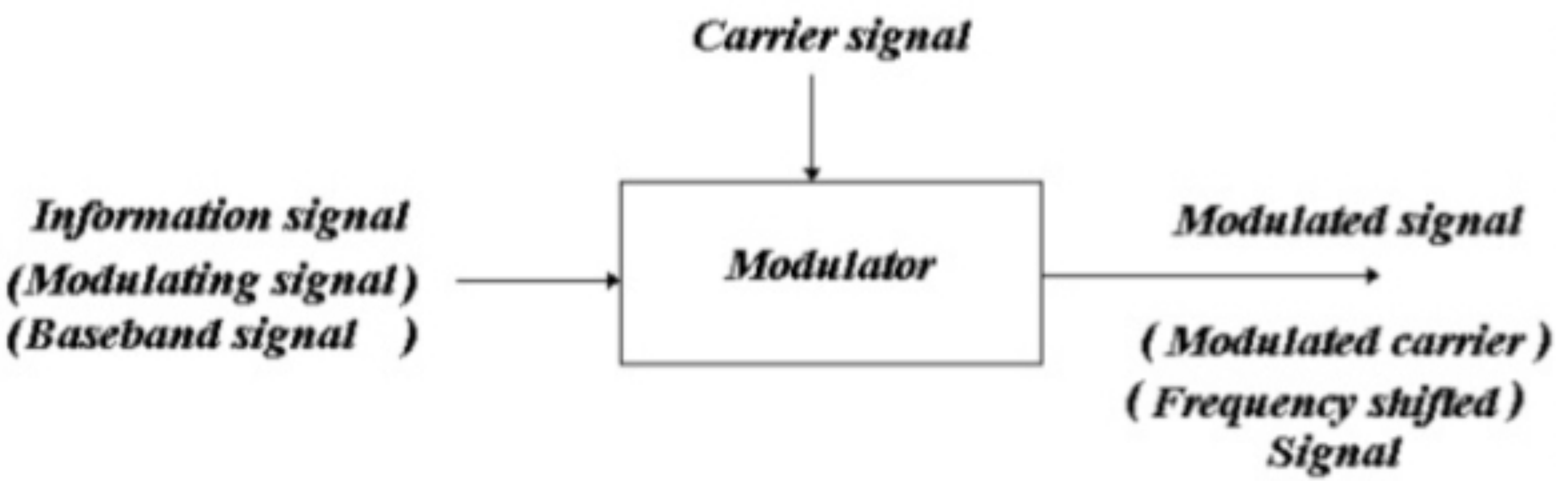

Different Modulation Methods

ANALOG Modulation

- Modulating signal and Carrier are both analog

- TYPES
  - Amplitude Modulation (AM)
  - Frequency Modulation (FM)
  - Phase modulation (PM)

====================================

- DIGITAL demodulation
  - Modulating signal is digital, while the carrier is analog
- TYPES
  - Amplitude Shift Keying (ASK)
  - Frequency Shift Keying (FSK)
  - Phase Shift Keying (PSK)

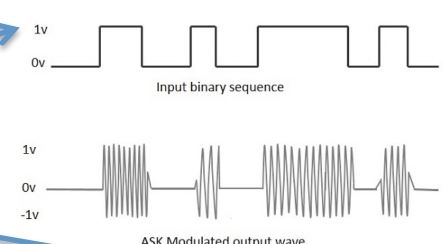

Binary Frequency Shift K.

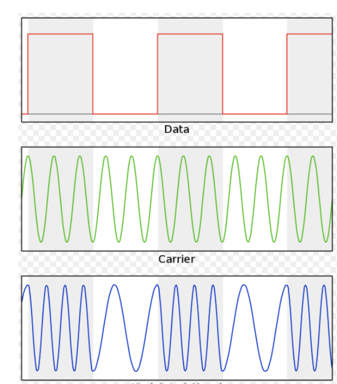

Amplitude Modulation

The simplest and earliest form of modulation

$$E(t) = A_c[1 + K\ m(t)]\cos(\omega_o t + \vartheta)$$

Non-linear process

$$m(t) = A_m \cos(\Omega t + \phi)$$

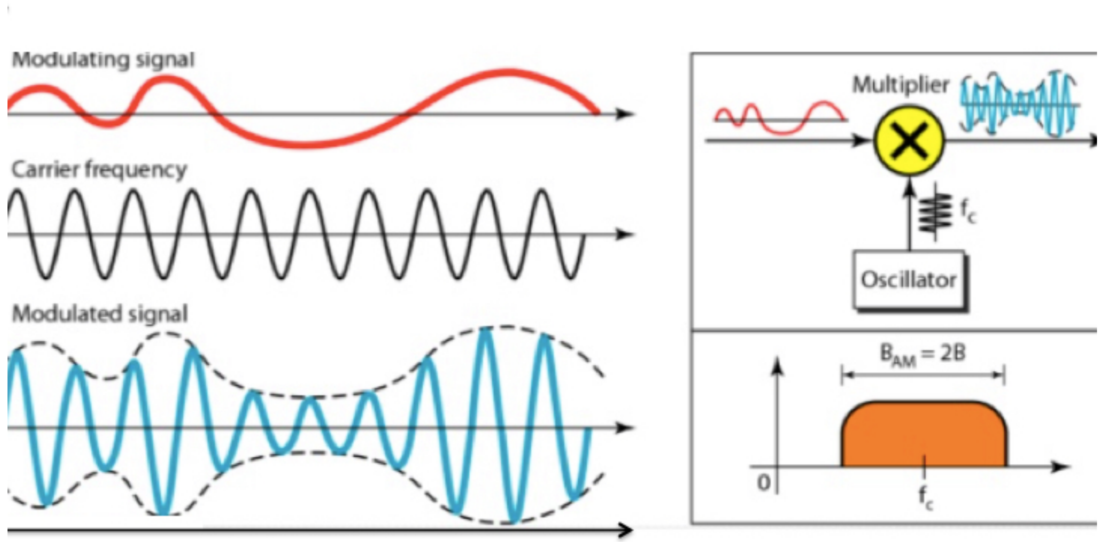

Spectrum

Typical limitation for sound transmission narrow bandwidth

Bandwidth ➔ $\Delta\omega = 2\Omega$

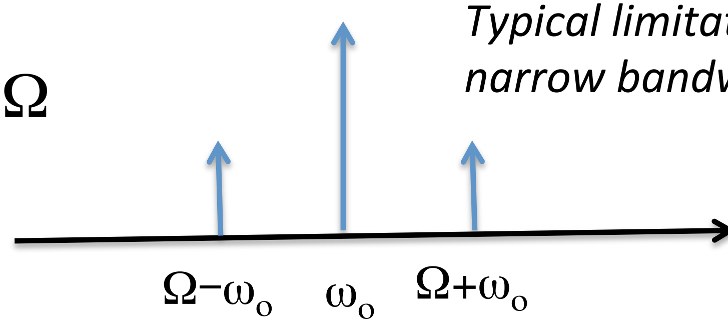

Frequency (FM) and Phase (PM) Modulation

- FM the carrier's frequency vary with the signal's input voltage
- PM the carrier's phase vary with the signal's input voltage

Two types of angle modulation schemes they differ from each other in terms of their respective transmission bandwidth

The simplest single frequency phase modulation:

$$E(t) = \mathcal{E}_0 \cos[\omega_o t + \delta_m \cos(\Omega t + \phi_m)] \quad \text{with } \Omega \ll \omega_0 \text{ and } \delta_m \ll 1$$

Complex representation of the modulated amplitude of the carrier

$$\mathcal{E}_0 \, (1/\sqrt{2}\,) \, \exp[\, i\, \delta_m \cos(\Omega t + \phi_m)]$$

Quadrature,

$$\mathcal{E}_c(t) \simeq \mathcal{E}_0 \qquad \mathcal{E}_s(t) \simeq \delta_m \mathcal{E}_0 \cos(\Omega t + \varphi_m)$$

Note: ***only the sine quadrature to the respect of the carrier contains the modulation signal***

PM spectrum

$$\mathcal{E}_0\ (1/\sqrt{2})\ \exp[\,i\,\delta_m \cos(\Omega t+\phi_m)]\ \simeq$$

$$\simeq\ J_o(\delta_m) + i(\,J_1(\delta_m)\,e^{i(\Omega t+\phi_m)} + J_{-1}(\delta_m)\,e^{-i(\Omega t+\phi_m)}\,] + \ldots\ldots\ldots\ldots$$

with

$$J_o(\delta_m) \simeq 1 \qquad J_1(\delta_m) = J_{-1}(\delta_m) \simeq \delta_m/2$$

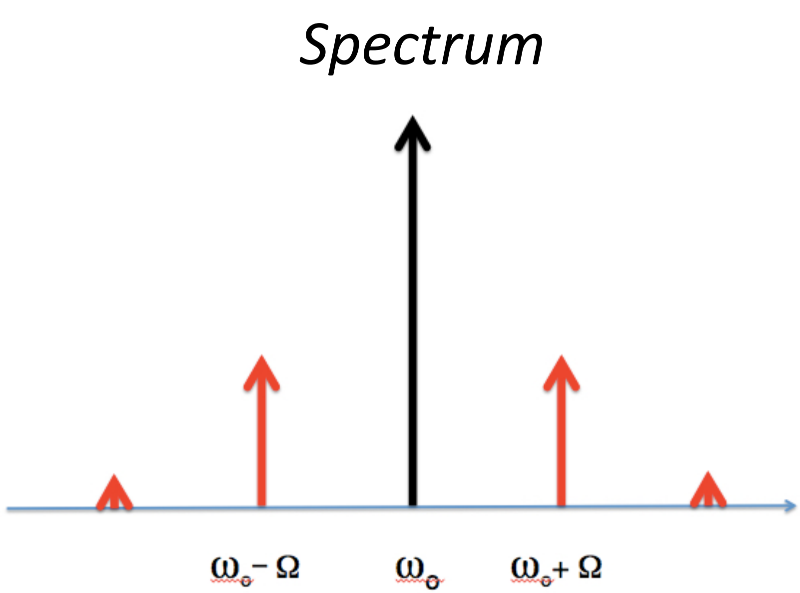

PM in the complex plane

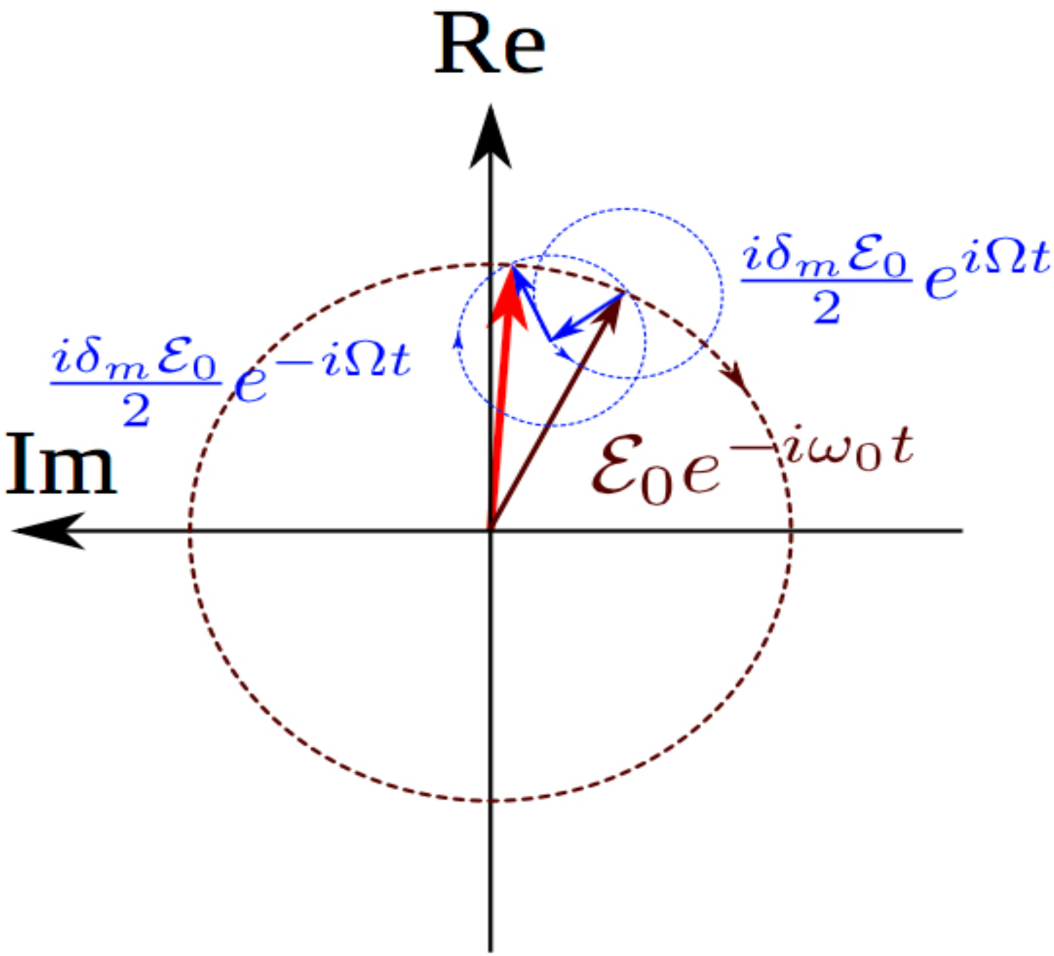

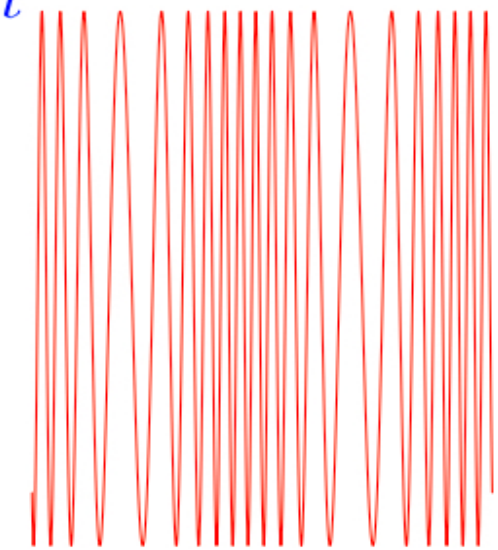

The resulting modulated oscillation vector (red arrow) has approximately the same length as the carrier field vector but outruns or lags behind the latter periodically with the modulation frequency Ω.

Photodiode and Modulation

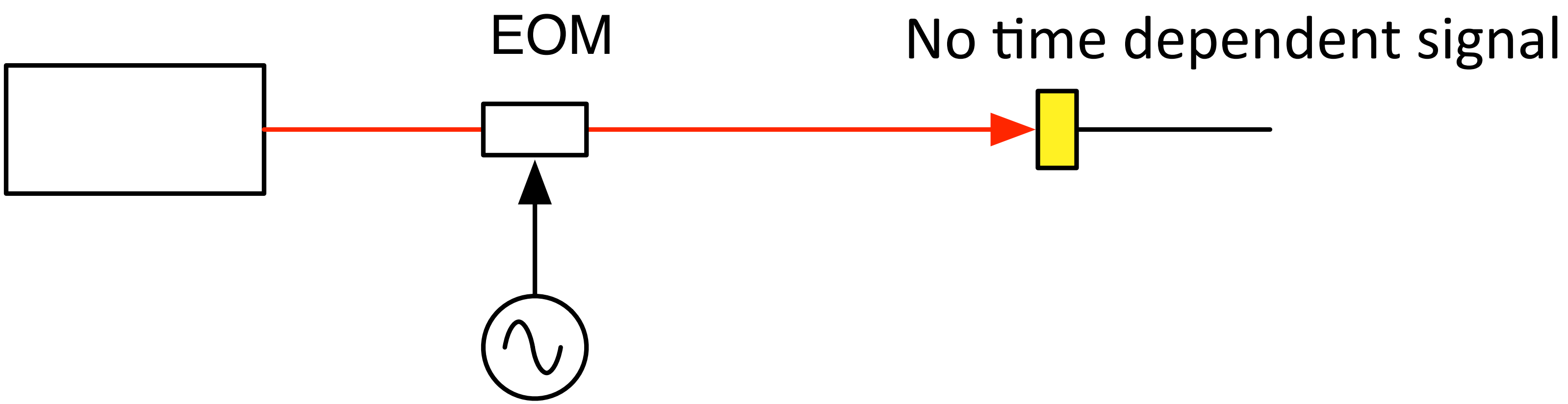

$$EE^* = E_{\rm in}^2 e^{i(-\Omega t + m\cos\omega_{\rm m} t)} e^{-i(-\Omega t + m\cos\omega_{\rm m} t)}$$
$$= E_{\rm in}^2 \quad (\text{constant})$$

Note: Photodetectors don't feel phase modulation!

How to detect modulation component

- PM detection must start before the photodetector: interfere the phase-modulated signal (*target beam*) with another signal (the *local oscillator* acting as a phase reference), prior to photodetection.
- *Local oscillator and Target beam* combine like an amplitude modulation to produce a detectable oscillation
  - ***Homodyne detection***: local oscillator and target beam have the same frequencies
  - ***Heterodyne detection***: local oscillator and target beam have different frequencies (frequency-shifted local oscillator beam, which beats with each individual sideband in the target beam with a different beat frequency)

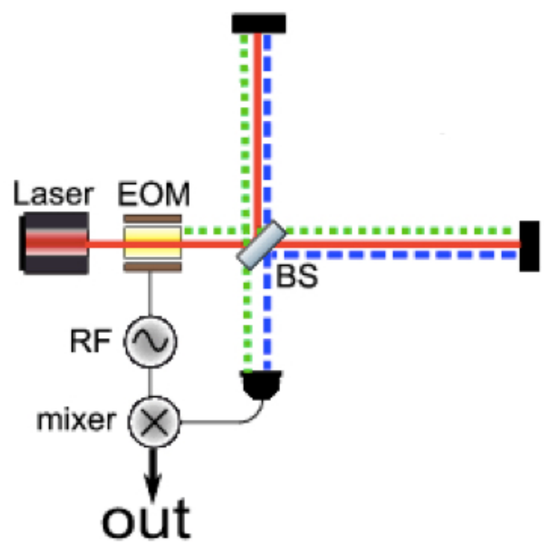

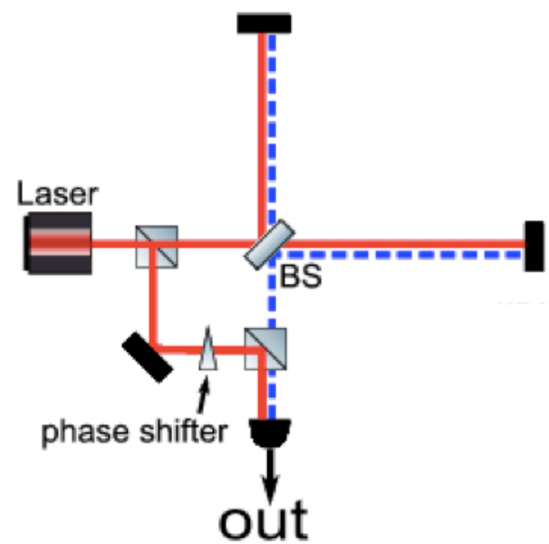

Optical Elements (OP)

- Mirror and Beam Splitter → linear systems with two input and two output ports

$r^2 = R$ → Reflectivity $t^2 = T$ → Trasmittivity   *in absence of loss*
$R+T=1$

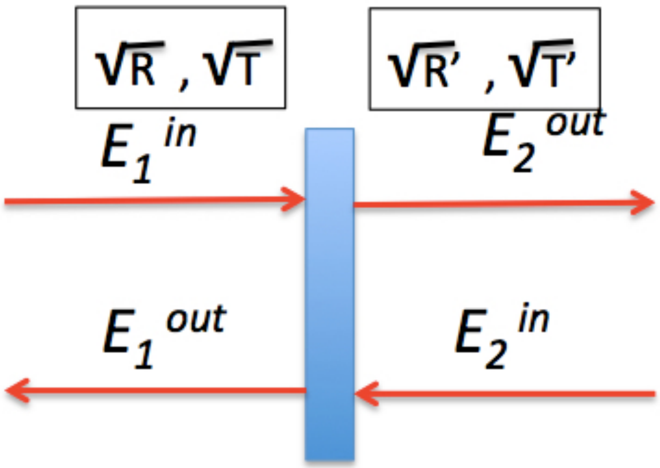

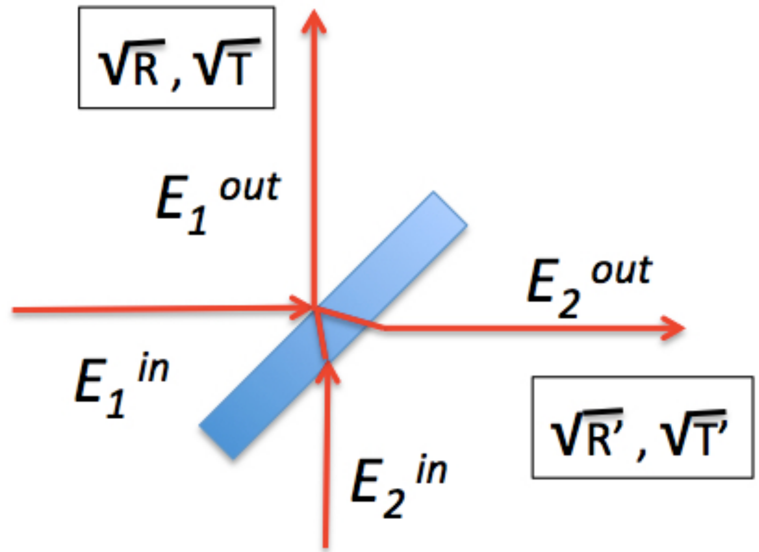

$$E_1^{out} = -\sqrt{R}\, E_1^{in} + \sqrt{T}\, E_2^{in}$$

$$E_2^{out} = \sqrt{R'}\, E_2^{in} + \sqrt{T'}\, E_1^{in}$$

$$E_1^{out} = \sqrt{T'}\, E_2^{in} - \sqrt{R}\, E_2^{in}$$

$$E_2^{out} = \sqrt{R'}\, E_2^{in} + \sqrt{T}\, E_1^{in}$$

OP formal representation

Mirror: Input – output electric fields connected via the Mirror Matrix M

$$M = \begin{pmatrix} -\sqrt{R} & \sqrt{T} \\ \sqrt{T} & \sqrt{R} \end{pmatrix}$$

Mirror : electric field quadrature components

$$\begin{pmatrix} \mathcal{E}^{out}_{1c} \\ \mathcal{E}^{out}_{1s} \\ \mathcal{E}^{out}_{2c} \\ \mathcal{E}^{out}_{2s} \end{pmatrix} = \begin{pmatrix} -\sqrt{R} & 0 & \sqrt{T} & 0 \\ 0 & -\sqrt{R} & 0 & \sqrt{T} \\ \sqrt{T} & 0 & \sqrt{R} & 0 \\ 0 & \sqrt{T} & 0 & \sqrt{R} \end{pmatrix} \begin{pmatrix} \mathcal{E}^{in}_{1c} \\ \mathcal{E}^{in}_{1s} \\ \mathcal{E}^{in}_{2c} \\ \mathcal{E}^{in}_{2s} \end{pmatrix}$$

50% Beam Splitter : matrix for transforming electric field quadrature components

$$M_{50\%,50\%} = \begin{pmatrix} -\sqrt{\frac{1}{2}} & 0 & \sqrt{\frac{1}{2}} & 0 \\ 0 & -\sqrt{\frac{1}{2}} & 0 & \sqrt{\frac{1}{2}} \\ \sqrt{\frac{1}{2}} & 0 & \sqrt{\frac{1}{2}} & 0 \\ 0 & \sqrt{\frac{1}{2}} & 0 & \sqrt{\frac{1}{2}} \end{pmatrix}$$

Mirror Motion (I)

$$M = \begin{pmatrix} -\sqrt{R} & \sqrt{T} \\ \sqrt{T} & \sqrt{R} \end{pmatrix}$$

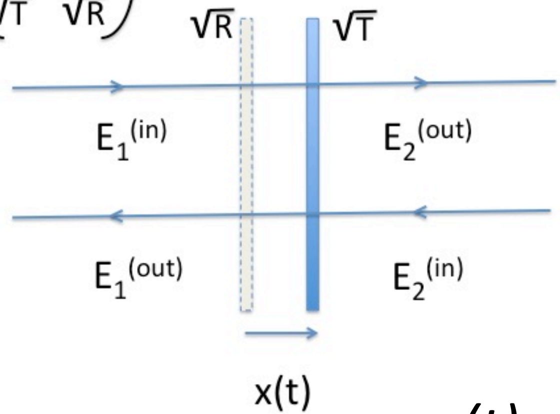

$$E_1^{(out)}(t) = -\sqrt{R}E_1^{(in)}(t - 2x(t)/c) + \sqrt{T}E_2^{(in)}(t)$$

$$E_2^{(out)}(t) = \sqrt{T}E_1^{(in)}(t) + \sqrt{R}E_2^{(in)}(t + 2x(t)/c)$$

$$x(t) << \omega /(2\,\pi\, c\ )$$

The output electric fields are phase modulated by the mirror motion

The modulation effect is encoded just in the s-quadrature of the electric field.

The light spectral component $L_s(\Omega)$ containing information of the motion x (with spectral component $X(\Omega)$) is proportional to the incoming light $\mathcal{E}_0$

$$L_s(\Omega) = (\omega_0/2\,\pi\, c)\ \ X(\Omega)\ \ \mathcal{E}_0$$

Mirror Motion (II)

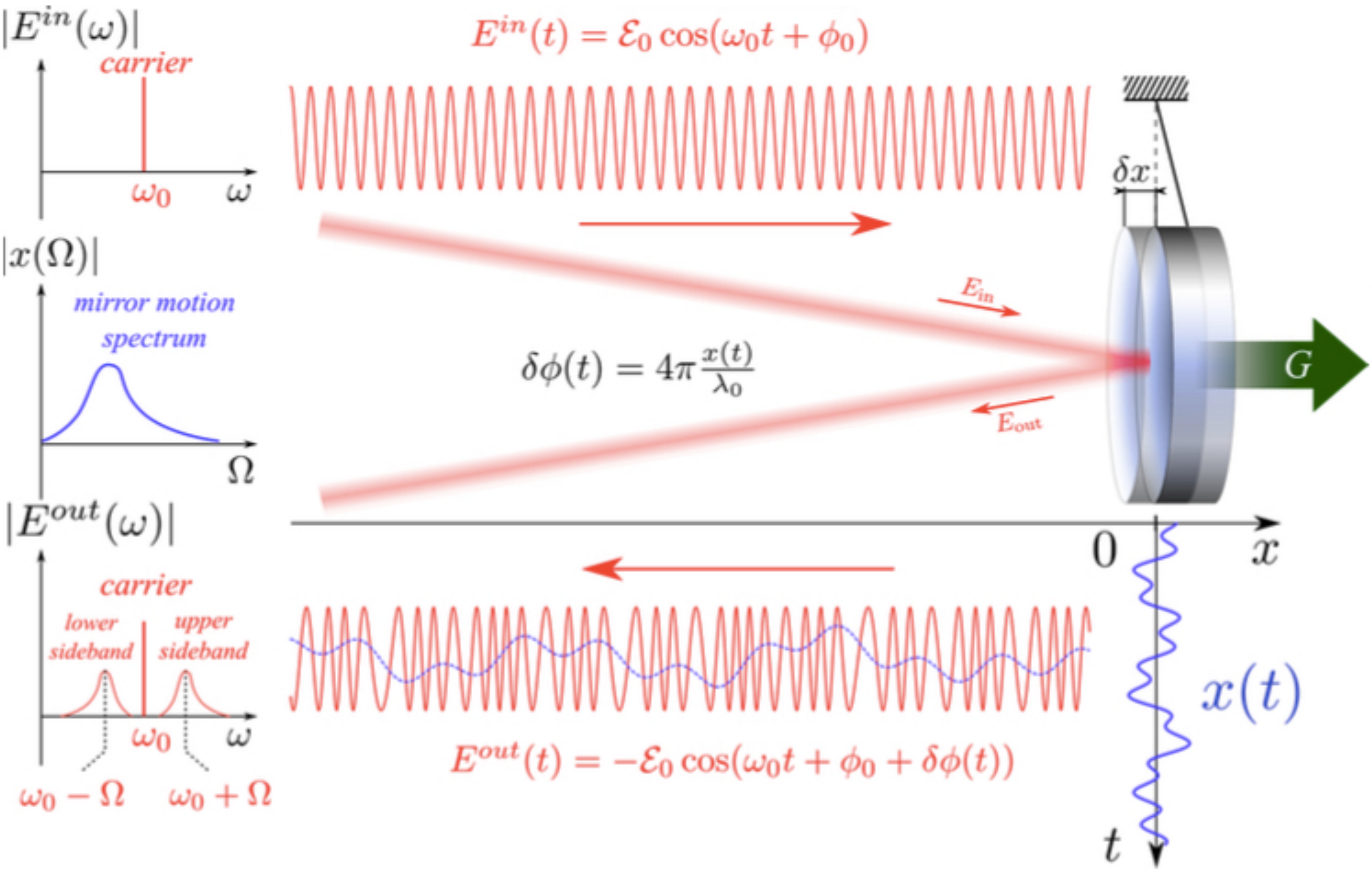

The MICHELSON Interferometer

Michelson Interferometer

Two different mirrors : $r_1 = \sqrt{R_1} \neq r_2 = \sqrt{R_2}$

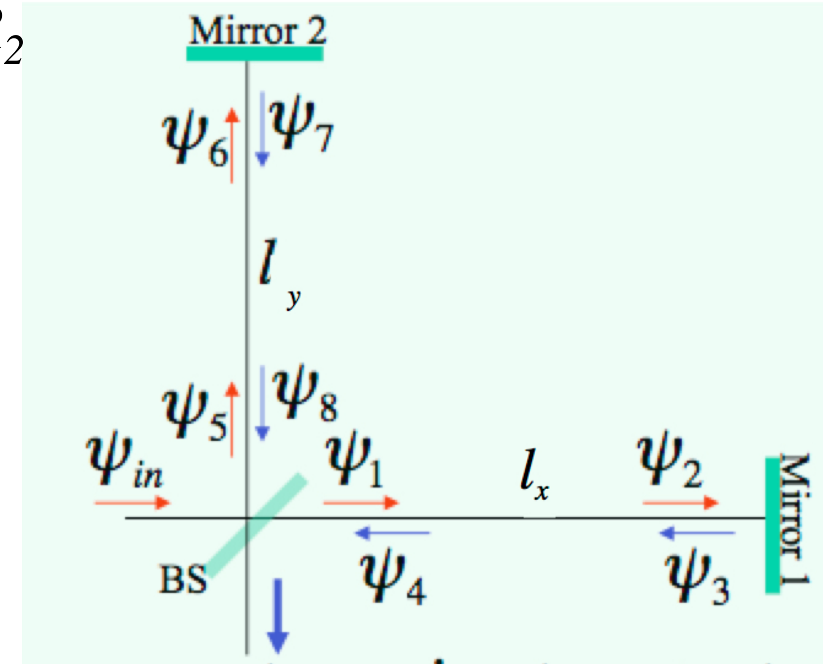

$$\psi_{in} = Ke^{i\chi}$$

$$\psi_1 = t_{BS}\psi_{in} \qquad \psi_5 = ir_{BS}\psi_{in}$$

$$\psi_2 = e^{-ikl_1}\psi_1 \qquad \psi_6 = e^{-ikl_2}\psi_5$$

$$\psi_3 = ir_1\psi_2 \qquad \psi_7 = ir_2\psi_6$$

$$\psi_4 = e^{-ikl_1}\psi_3 \qquad \psi_8 = e_2^{-ikl}\psi_7$$

$$\psi_{out} = ir_{BS}\psi_4 + t_{BS}\psi_8$$

$$\left|\psi_{out}\right|^2 = \mathrm{P}_{in}\mathrm{r}_{BS}^2\, t_{BS}^2 (r_1^2 + r_2^2)\left[1 + \frac{2r_1r_2}{r_1^2 + r_2^2}\cos\left(2k\delta l\right)\right]$$

$$\delta l = l_x - l_y$$

$$C = constrast = \frac{2r_1r_2}{r_1^2 + r_2^2} = \frac{P_{out}^{\max} - P_{in}^{\min}}{P_{out}^{\max} + P_{in}^{\min}}$$

Michelson Interferometer and GW

At the dark fringe with $l_x = l_y$ for all light frequencies the output is zero (zero frequency noise)

In absence of a modulation signal the electric field at the output of an interferometer operated on a dark fringe

GW perturbs the arm length $h << l$

$$r_1 = r_2 = \sqrt{R}$$

$$\Psi_{out} = -\Psi_{in}\frac{1}{2}\sqrt{R}[e^{i2\frac{\omega_o l_x}{c}} - e^{i2\frac{\omega_o l_y}{c}}]$$

$$l = \frac{l_x + l_y}{2}$$

$$h = \frac{\delta l_x - \delta l_x}{l} << 1$$

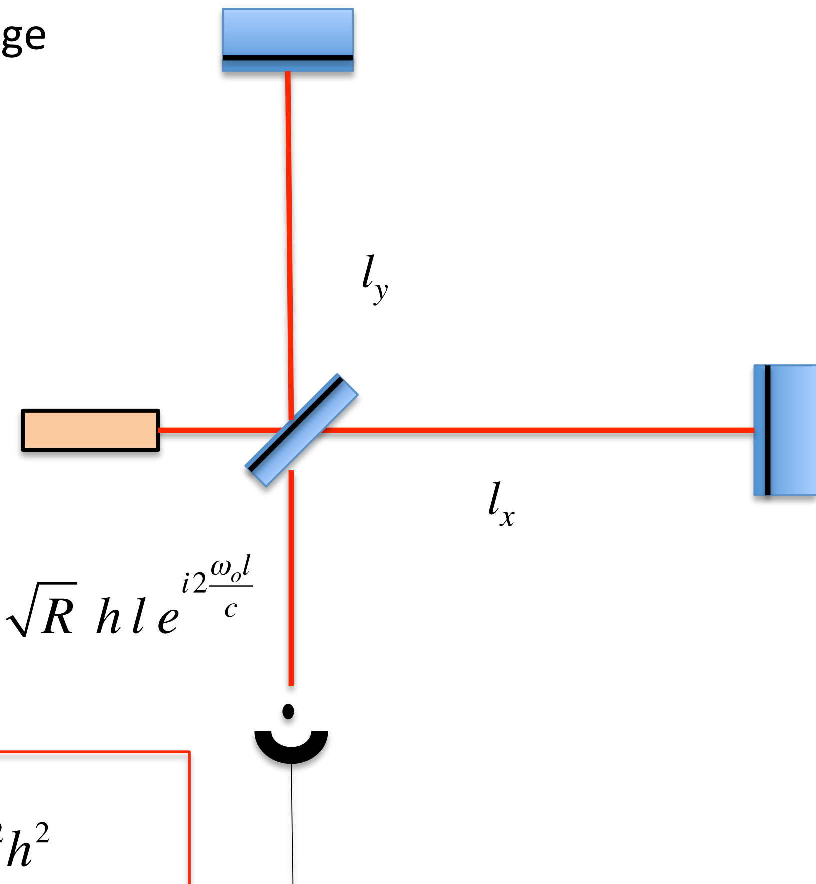

$$\Psi_{out} \approx -i\,\Psi_{in}\frac{\omega_o}{c}\sqrt{R}\;h\,l\,e^{i2\frac{\omega_o l}{c}}$$

$$P_{out} \approx P_{in}\left(\frac{\omega_o}{c}\right)^2 l^2 h^2$$

The photodiode output depends on h² ➔ *detection impossible*

Michelson Lock on Dark fringe

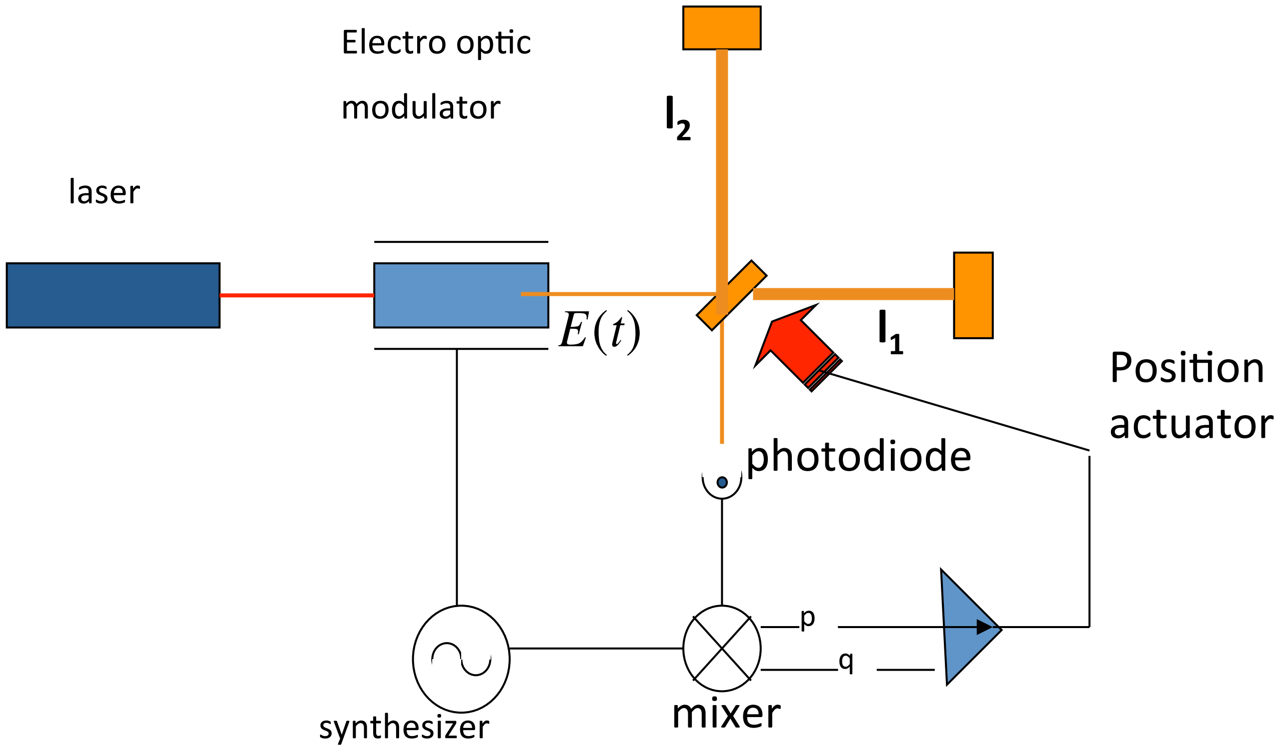

Field at the input of the modulator $\Psi_{in}(t) = A_0 e^{i\omega_0 t}$

Field at the modulator output

$$\Psi_{in}^{m}(t) = E_0 \cdot e^{i(\omega_0 t + \delta_m \sin \Omega t)} \approx E_0 (J_0(\delta_m) e^{i\omega_0 t} + J_1(\delta_m) e^{i(\omega_0 + \Omega)t} - J_1(\delta_m) e^{-i(\omega_0 - \Omega)t})$$

Michelson length control

- Michelson is operated at the dark fringe

At the dark fringe, DC signals can't be a good error signal

– Schnupp asymmetry:

Introduce small arm length asymmetry

=> RF sidebands leaks to the dark port

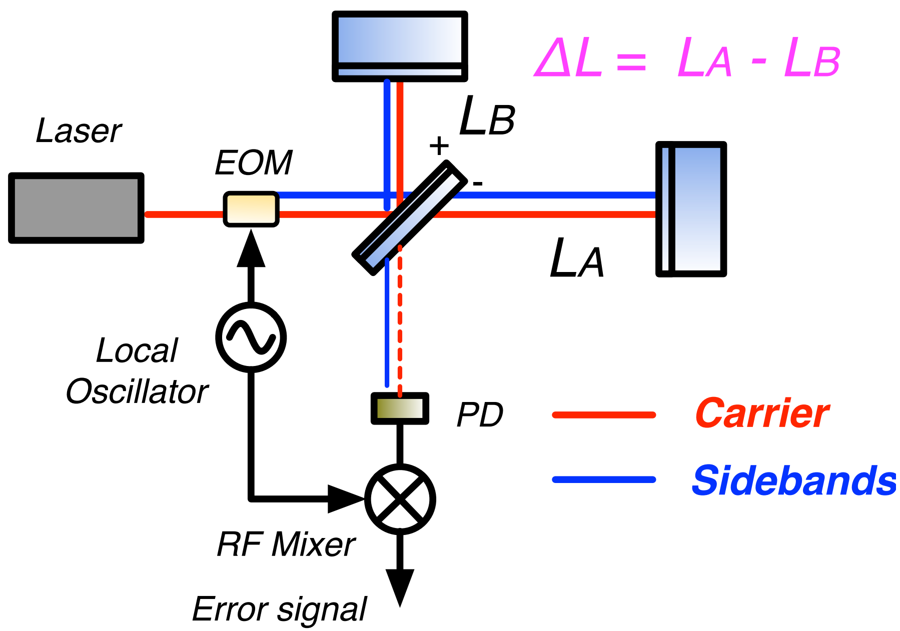

Schnupp asymmetry & sideband picture

- Because of the asymmetry, the output port is no longer dark for the sidebands even if the carrier is at dark.

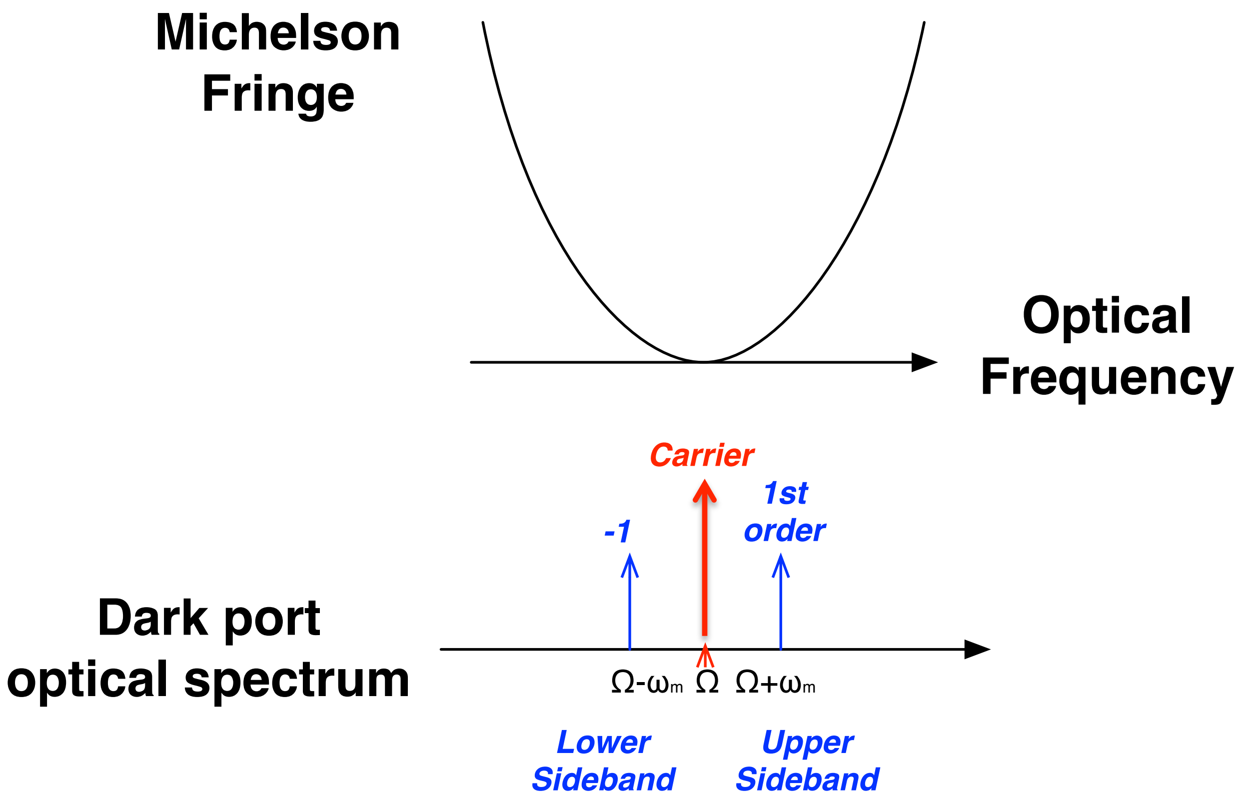

Sidebands and phasor picture

- In presence of the Schnupp asymmetry

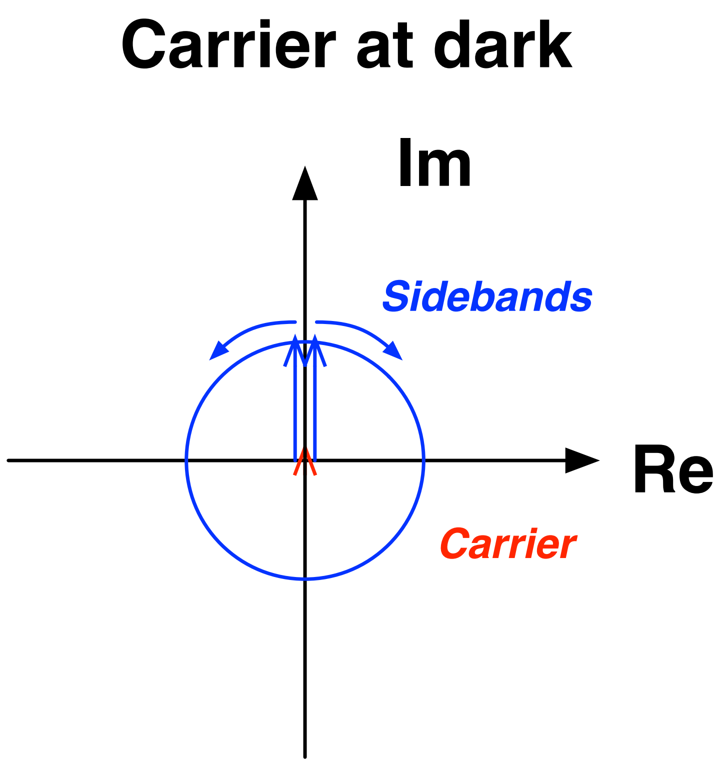

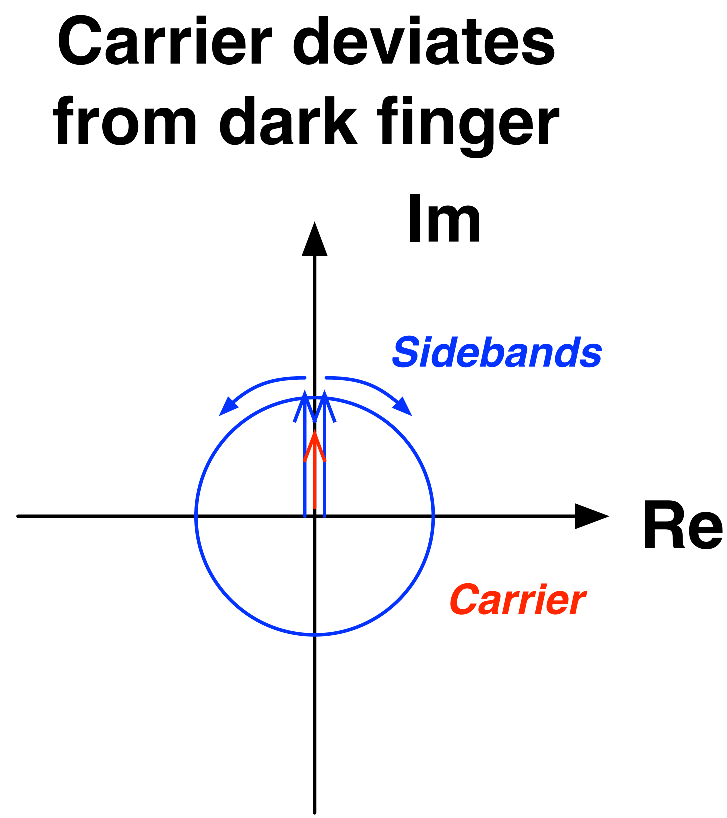

The role of the Schnupp asimmetry

The interferometer output is set equal zero for the carrier component –dark fringe –insensitive to the noise (but also to the GW signal). Let us add modulation and a difference in the arms

$$\Psi^m_{out}(t) = [A_c\Psi_0 + A_+\Psi_+ e^{i\Omega t} + A_-\Psi_- e^{-i\Omega t}]e^{i\omega_0 t}$$

$$\Delta l_{Sc} = l_x - l_y \qquad \delta l_{gw} = l\ h$$

$$\delta l = \delta l_{gw} + \Delta l_{Sc}$$

$$\Psi^m_{out}(t) = i\Psi_{in} e^{i\frac{\omega_o}{c}l}[J_o l\ h\ \frac{\omega_o}{c} + 2J_1 \sin(\frac{\Omega}{c}\Delta l_{Sc})\cos(\Omega t + 2\frac{\Omega}{c}l)]$$

PHD output:

$$P_{out} \approx P_{in}\{J_0^2(\frac{\omega_o}{c})^2 l^2 h^2 + 2J_1^2\frac{\omega_0}{c}[1+\cos(2\Omega t + 4\frac{\Omega}{c}l)]\sin^2(\frac{\Omega}{c}\Delta l_{Sc}) + 2J_o J_1\frac{\omega_0}{c} l\ h\cos(\Omega t + 2\frac{\Omega}{c}l)]\sin\ (\frac{\Omega}{c}\Delta l_{Sc})\}$$

A Schnupp asymmetry of the arms is needed

h the GW signal can appear in the phase component at Ω

The Fabry-Perot Interferometer

The simple Fabry-Perot: basic formalism (I)

$$\psi_{in} = Ke^{i\chi}$$

$$\psi_1 = unknown$$

$$\psi_2 = e^{-ikl}\psi_1$$

$$\psi_3 = ir_2\psi_2$$

$$\psi_4 = e^{-ikl}\psi_3$$

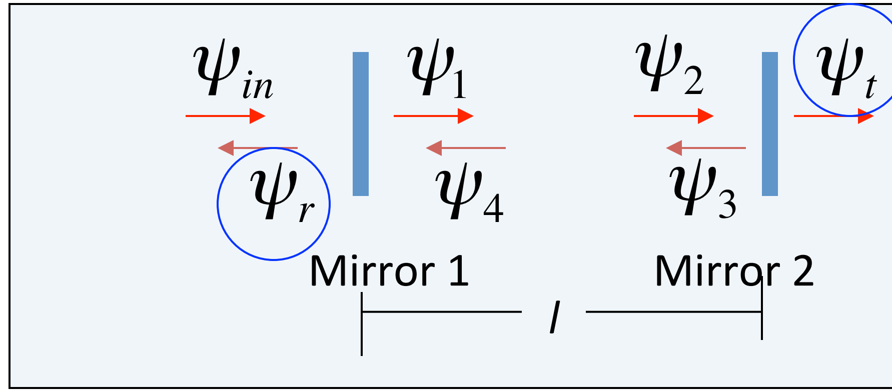

steady state: $\psi_1 = t_1\psi_{in} + ir_1\psi_4$ ⟹

$$\psi_1 = \frac{t_1}{1 + r_1 r_2 e^{-2ikl}}\psi_{in}$$

$$\psi_4 = \frac{ir_2 t_1}{1 + r_1 r_2 e^{-2ikl}}\psi_{in}$$

Reflected wave: $\psi_r = ir_1\psi_{in} + t_1\psi_4 = i\dfrac{r_1 + r_2 e^{-2ikl}}{1 + r_1 r_2 e^{-2ikl}}\psi_{in}$

Transmitted wave: $\psi_t = t_2\psi_2 = \dfrac{t_1 t_2 e^{-ikl}}{1 + r_1 r_2 e^{-2ikl}}\psi_{in}$

FP basic formalism (II)

Wave amplitudes:

$$|\psi_r|^2 = |A_r|^2 \qquad A_r = \sqrt{\frac{r_1^2 r_2^2 + 2r_1 r_2 \cos 2kl}{1 + r_1^2 r_2^2 + 2r_1 r_2 \cos 2kl}}$$

$$|\psi_t|^2 = |A_t|^2 \qquad A_t = \sqrt{\frac{1}{1 + r_1^2 r_2^2 + 2r_1 r_2 \cos 2kl}}\, t_1 t_2$$

if :

$$L = (2m+1)\frac{\lambda}{4} \Longrightarrow A_r = \min = \frac{r_2 - r_1}{1 - r_1 r_2}; A_t = MAX = \frac{t_1 t_2}{1 - r_1 r_2}$$

$$L = m\lambda \Longrightarrow A_r = MAX = \frac{r_2 + r_1}{1 + r_1 r_2}; A_t = \min = \frac{t_1 t_2}{1 + r_1 r_2}$$

The light resonates into the cavity if its phase is increased by exactly 2π each two reflections

FP basic formalism (III)

Main cavity features

Finesse: $$F = \frac{FSR}{FWHM} \approx \frac{\pi\sqrt{r_1 r_2}}{1 - r_1 r_2}$$

full width @ half max

where

Free Spectral Range: $$FSR = \frac{c}{2L} = \Delta\nu_{FSR}$$

$$FSR = \Delta\lambda_{FSR} = \frac{\lambda^2}{2L}$$

note

Round trip number: $$N = \frac{F}{2\pi}$$

Cavity cut-off: $$\omega_c = 2\pi\frac{FWHM}{2} = \pi\frac{c}{2FL} = \frac{1}{\tau_s}$$

Storage time

Recycling factor : $$FI = \left|\frac{\psi_{3;L=(2m+1)\frac{\lambda}{4}}}{\psi_{in}}\right| = \frac{t_1^{\;2}}{(1 - r_1 r_2)^2}$$

FP Airy function

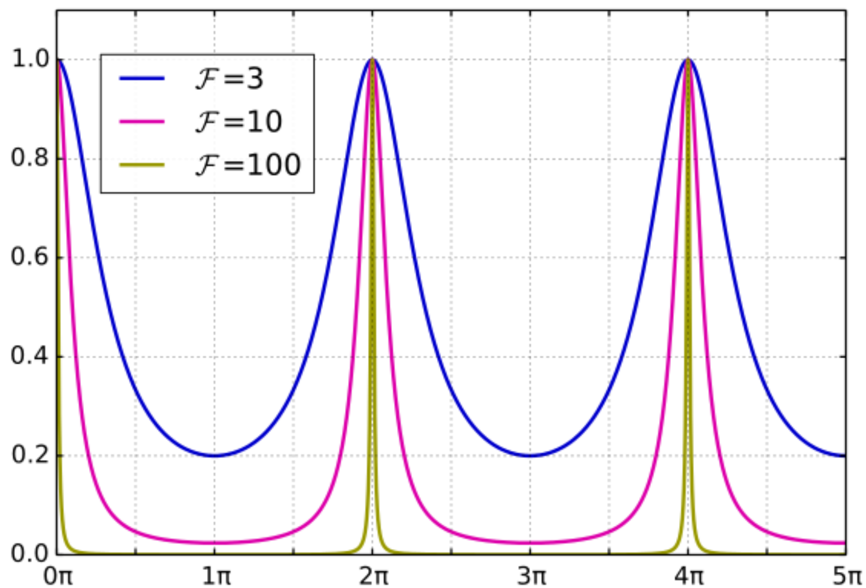

$\delta\lambda$ ➔ bandwidth

Finesse = F = $\Delta\lambda_{FSR} / \delta\lambda$

$\Delta\lambda$ ➔ Free Spectral Range ➔ FSR

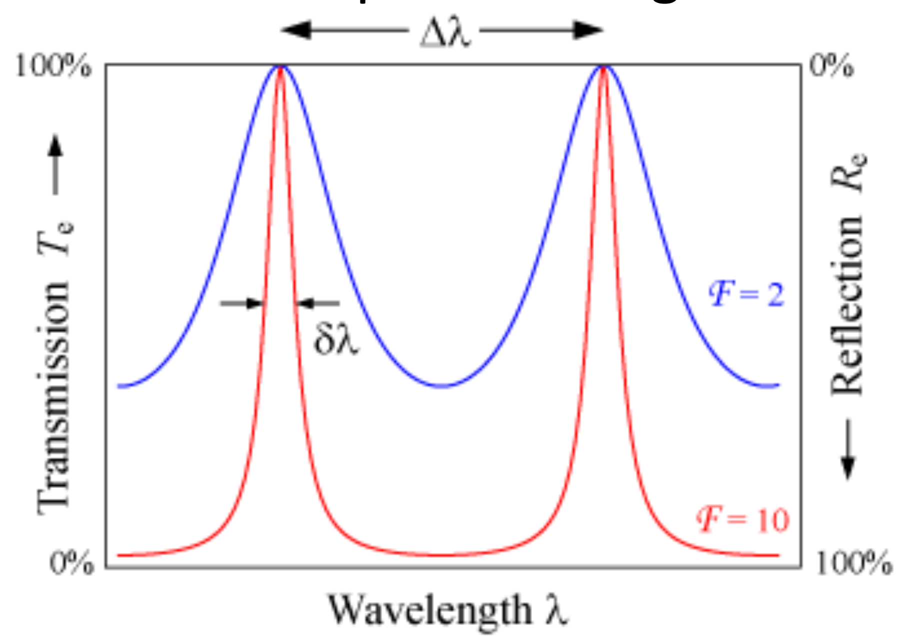

A numeric example:

$\lambda = 1\ \mu m$

FSR = $\lambda^2/2L = \frac{1}{2}(10^{-12} / 3\ 10^3) = 1.7\ 10^{-16}$

F=10

$\delta\lambda$ = $FSR/F \sim 1.7\ 10^{-17}\ m$

FP - transmission

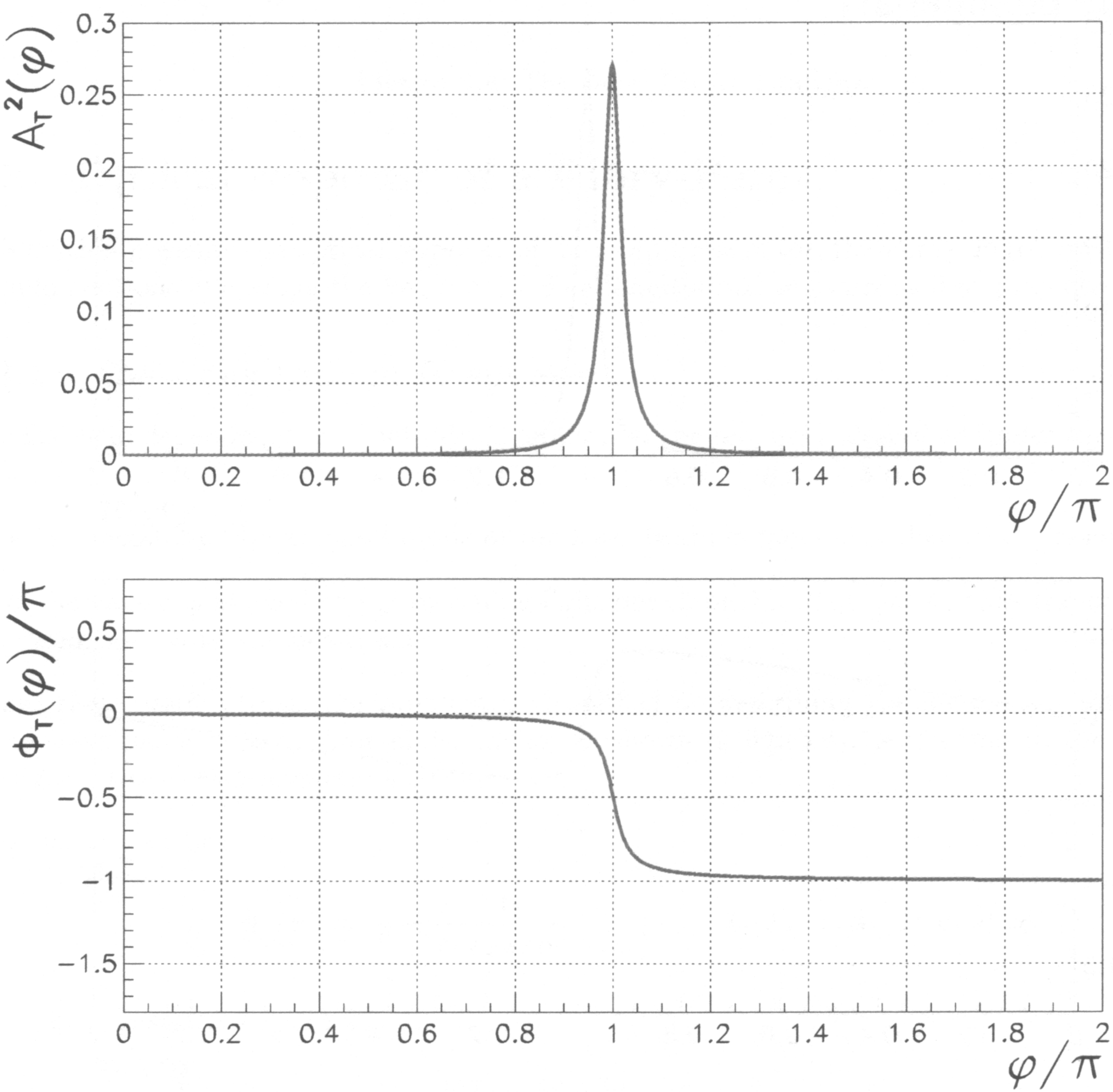

FP - reflection

$$\frac{\Psi_r}{\Psi_{in}} = i\,\frac{r_1 + r_2 e^{-2ikl}}{1 + r_1 r_2 e^{-2ikl}}$$

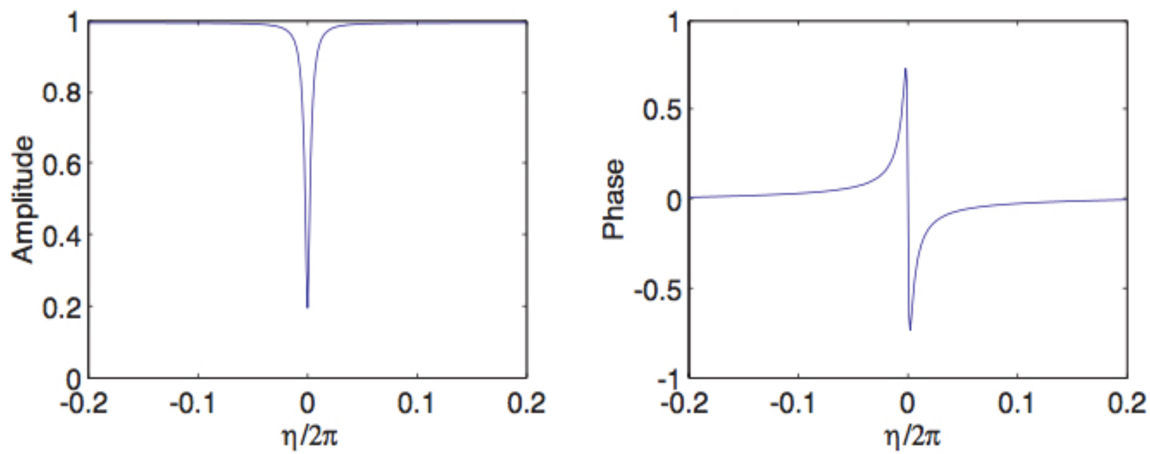

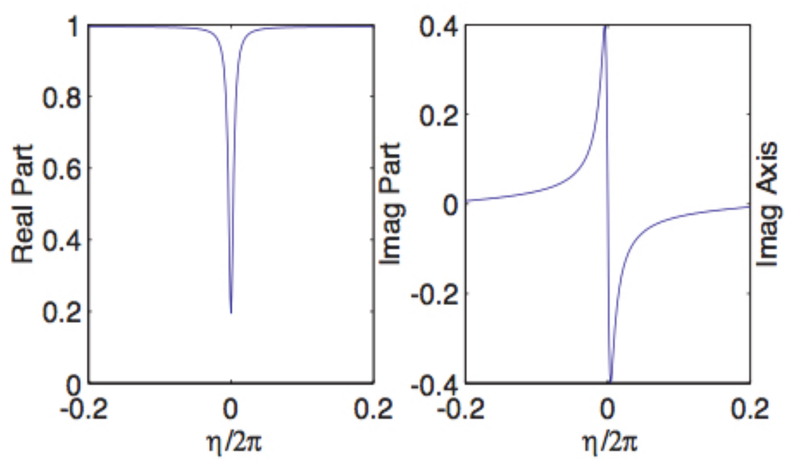

$\frac{\Psi_r}{\Psi_{in}}$ In a complex plane

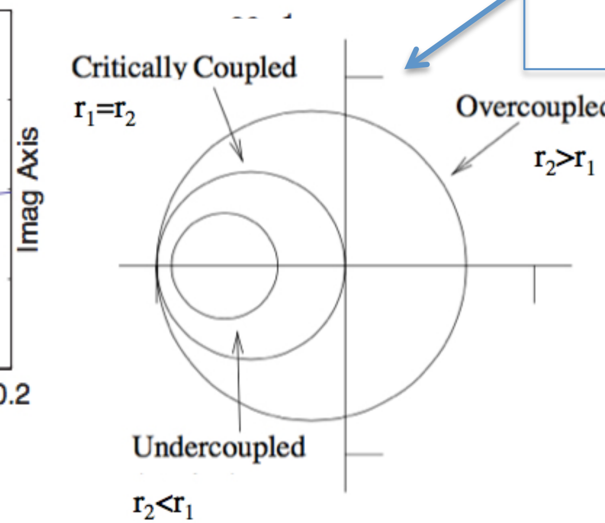

Over coupled cavity :almost all the light is reflected back by the cavity

FP basic formalism (IV)

Optical cavity length (depends on the frequency!!):

$$L_{opt} = FL\frac{2}{\pi}\frac{1}{\sqrt{1+(\omega/\omega_c)^2}}$$

Note: in an interferometer with FP cavities every flat noise into the system (e.g. shot noise) causes a departure linearly dependent on the frequency from the cavity cutoff.

FP-Michelson ITF

The formalism to compute Michelson output field for it is exactly the same of that adopted for the simple Michelson, once the simple mirror reflectivity has been replaced with FP cavity reflectivity:

$$r_1 = A^{(1)}{}_r \qquad r_2 = A^{(2)}{}_r$$

Laser beam/cavity basics (I)

$$\nabla^2 U(x,y,z) + k^2(x,y,z) = 0$$

Coherent monocromatic wave emitted by the source

Along *z*, Hermite-Gauss complete set:

$$U(x,y,z) = \frac{A_{mn}}{w(z)} H_m(\sqrt{2}\frac{x}{w(z)}) H_n(\sqrt{2}\frac{y}{w(z)}) \left[-\frac{x^2+y^2}{w^2(z)} - i\frac{k(x^2+y^2)}{2R(z)} - i(kz - \phi_{nm}) \right]$$

$$w^2(z) = w_o^2 \left[1 + (\frac{\lambda z}{\pi w_o^2})^2 \right]$$

beam divergence θ_∞

$$R(z) = z\left[1 + (\frac{\pi w_o^2}{\lambda z})^2 \right]$$

$$\phi = (m + n + 1) \ \arctan(\theta_\infty \frac{z}{w_0})$$

Laser beam/cavity basics (II)

In a mode-matched cavity, if the cavity is stable and R(z) and w(z) are the same after an arbitrary number of reflections,

$$\nu_0 = c/2d$$

TEM$_{mn}$ resonant condition

$$\nu = \nu_0 \left[(q+1) + \frac{1}{\pi}(m+n+1) \ \arccos\sqrt{(1-\frac{d}{R_1})(1-\frac{d}{R_2})} \right]$$

arb.integer — mode order — Cavity stability

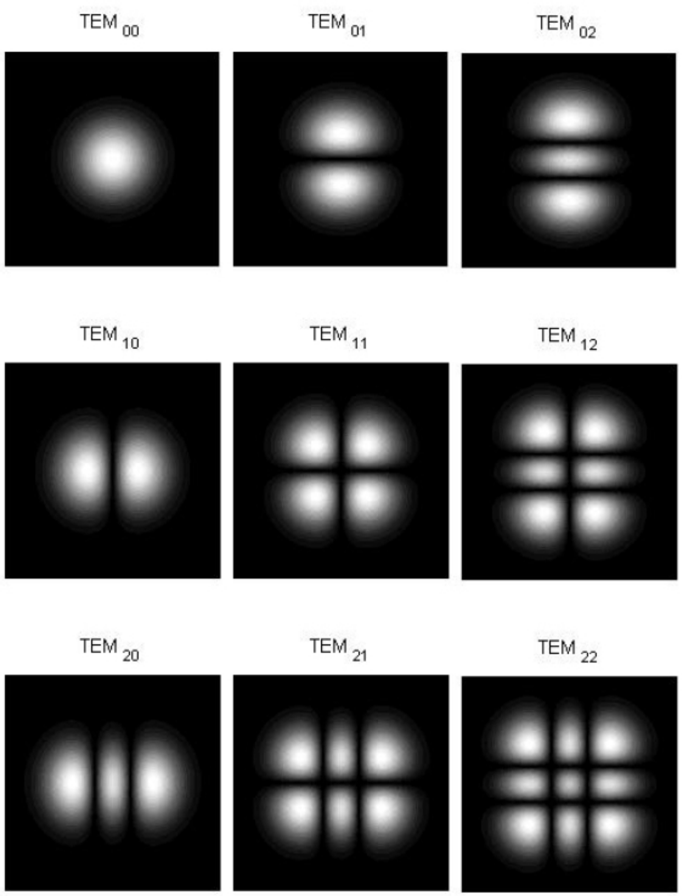

Longitudinal beam profile

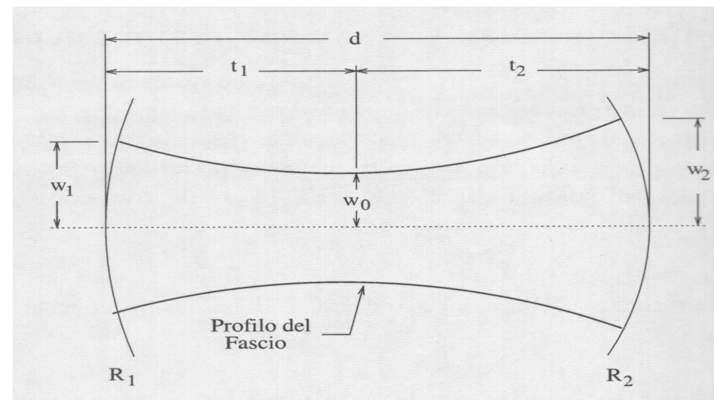

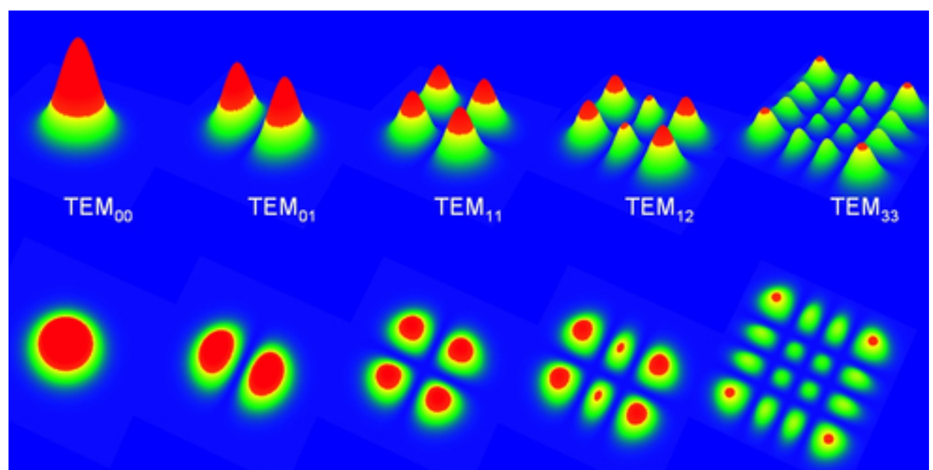

Optical Cavity Stability

Mirror Curvatures ρ_1 , ρ_2

Stability parameter ➔ $g_i = 1 - (L / \rho_i)$

with i=1,2 L=nL$_o$ and n intra-cavity refraction index

Stability Condition ➔ $0 \leq g_1 g_2 \leq 1$

Marginally stable cavities $g_1 g_2 = 1$

A cavity is stable if a ray launched inside the resonator parallel to the optical axis remains inside the resonator after an infinite number of bounces . If the ray is slightly off axis , it will be reflected in a direction to bring it back toward the center of the bore

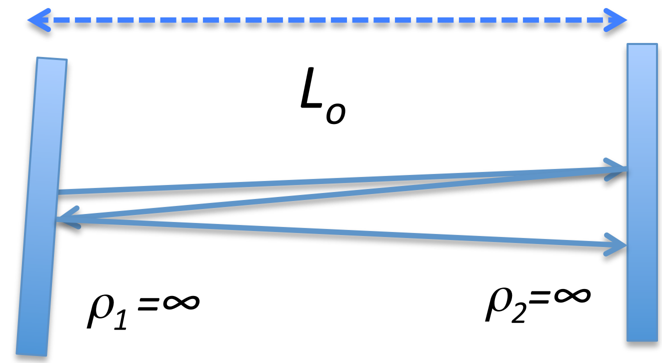

Conditionally stable
i.e. Stable if the mirrors are paralle

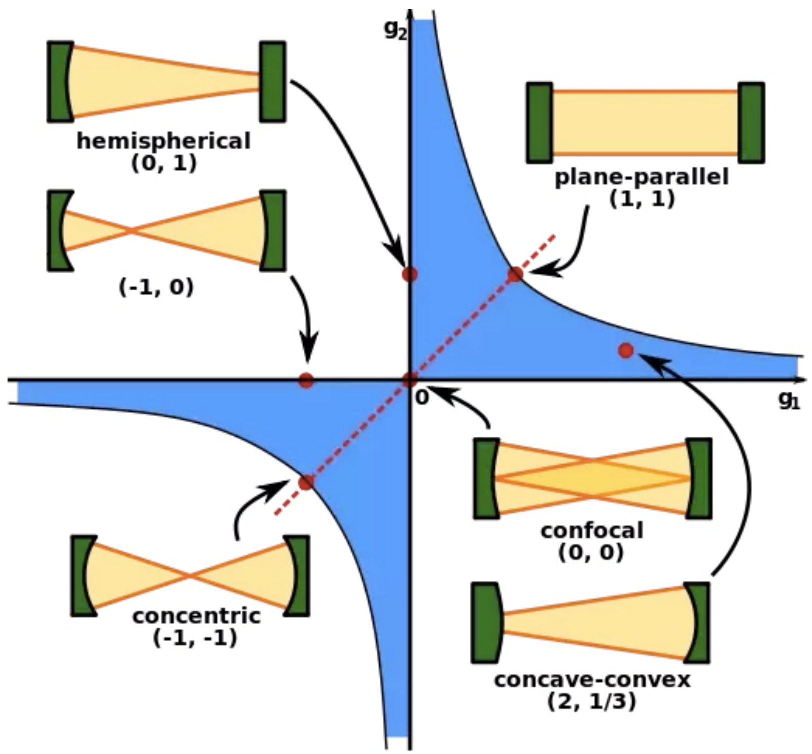

Lock of a single F-P cavity

In 1946 R. Pound defined the strategy, widely used in radio physics, that today is the standard method to stabilize the lasers and in general the optical cavities.

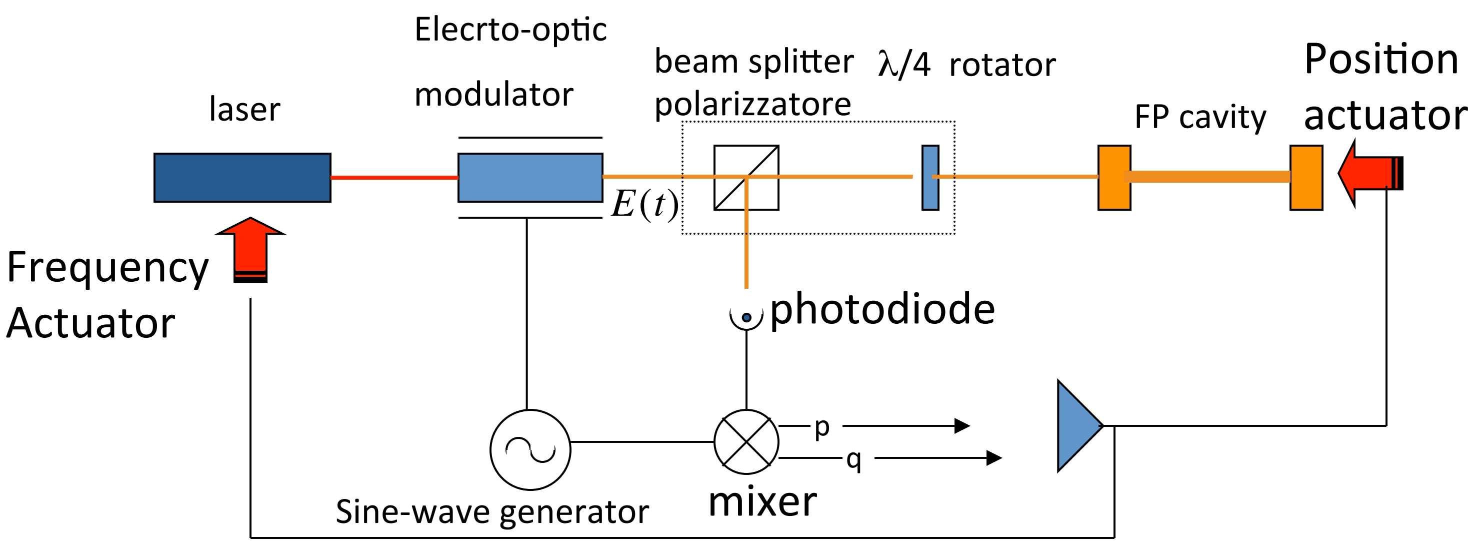

$$E(t) = E_0 \cdot e^{i(\omega_0 t + m\cos\Omega t)} \approx E_0\left(J_0(m)e^{i\omega_0 t} + J_1(m)e^{i(\omega_0+\Omega)t} - J_1(m)e^{i(\omega_0-\Omega)t}\right)$$

$$J_0(m) = 1; \quad J_1(m) = m/2$$

$$\mathrm{Re}\{E(t)\} = E_0\cos(\omega_0 t + m\cos\Omega t) \underset{m<<1}{\approx} E_0 \cdot \cos\omega_0 t - E_0 \sin\omega_0 t \cdot (m\cos\Omega t)$$

$$= E_0 \cdot \cos(\omega_0 t) - m\frac{E_0}{2}\sin(\omega_0 + \Omega)t - m\frac{E_0}{2}\sin(\omega_0 - \Omega)t + \ldots\ldots\ldots$$

Lock of a single F-P cavity

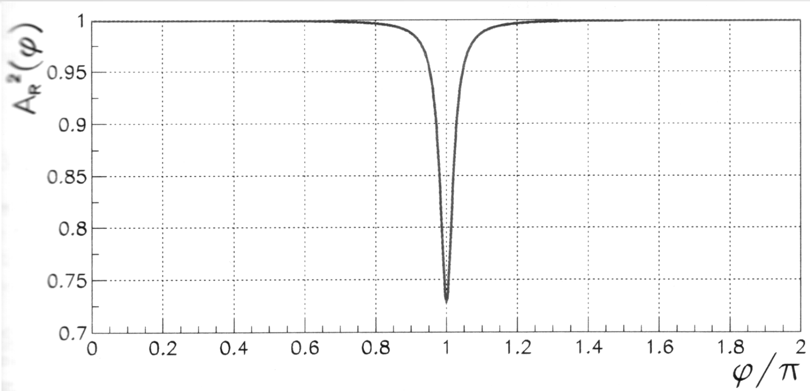

$$\psi_t = i\frac{r_1 + r_2 e^{-2ikl-2ikz\pm i2\frac{\Omega}{c}l}}{1 + r_1 r_2 e^{-2ikl-2ikz\pm 2i\frac{\Omega}{c}l}}\psi_{in}$$

The cavity length is set such that the carrier (ω_0) is resonant

$$e^{-2ikl} = -1$$

$$\psi_t = i\frac{r_1 - r_2 e^{-2ikz\pm i2\frac{\Omega}{c}l}}{1 - r_1 r_2 e^{-2ikz\pm 2i\frac{\Omega}{c}l}}$$

The side bands due to the modulation at Ω are anti-resonant {Ω = (N+1/2) (π c/l)}

$$e^{\pm 2\frac{\Omega}{c}l} = e^{\pm i\pi} \qquad \psi_t = i\frac{r_1 + r_2 e^{-2ikz}}{1 + r_1 r_2 e^{-2ikz}}\psi_{in}$$

When we have the perturbation of the cavity length z, i.e. $\phi_d = -2\,k\,z$:

Photo-diode output :

$$p = -4P_{in}J_0 J_1 r_2(1 + r_2^2) r_1 t_1^2 \frac{\sin 2kz}{1 + r_1^4 r_2^4 - 2r_1^2 r_2^2 \cos 4kz}$$

$$q = 0$$

The demodulated signal in phase at Ω contains the information on the length variation

Lock of a single FP cavity

If the FINESSE *F* >>1

$$\frac{dp}{dz} \cong J_o(\delta_m) J_1(\delta_m) P_{in} \frac{8F}{\lambda}$$

Higher FINESSE higher sensitive to length variation

Control dynamics

$$\delta z = \frac{1}{10} \frac{FWHM}{2} = \frac{\overbrace{\lambda/2}^{FSR}}{10 \cdot 2 \cdot F}$$

Control dynamics and linearity range reduced

Linearity Range

$$FWHM = \frac{\lambda}{2F}$$

PDH signals

Amplitude of the reflected light

Pound-Drever Signals

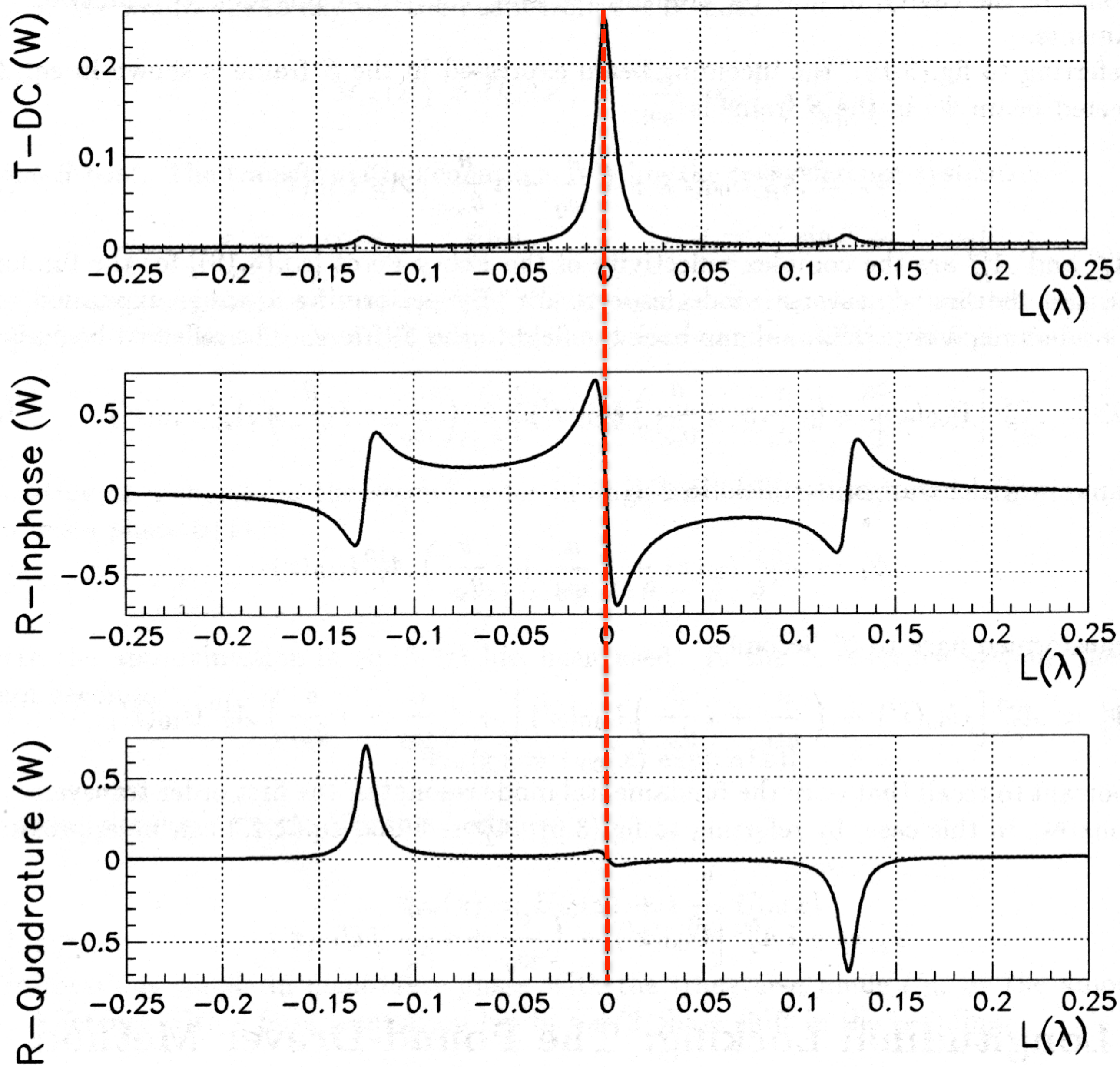

FP and GW signal

- Longer arms yield larger GW signals
- Increase the effective length of the arms by bouncing the light back and forth within them, or *folding* the beam
- *In a FP* kept near resonance, the phase of the output beam is very sensitive to the distance between the mirrors, consequence of the long storage time of the light into the cavity
- Light storage time $\tau_s = \frac{2}{\pi}\frac{FL}{c}$
- Equivalent number of bounces $N_{eq} = \frac{F}{2\pi}$

Michelson+Fabry-Perot

Mich.+F.P. and…. modulation

$l_{x,y}$ ➔ distance between the beam splitter and the first, or input (m range)

$L_x = L_y = L$ ➔ lengths of the Fabry-Perot cavities in the arms (km range)

$\Delta l_{Sc} = l_x - l_y$ Schnupp asymmetry ➔ between beamsplitter and arm cavities (tens of cm)

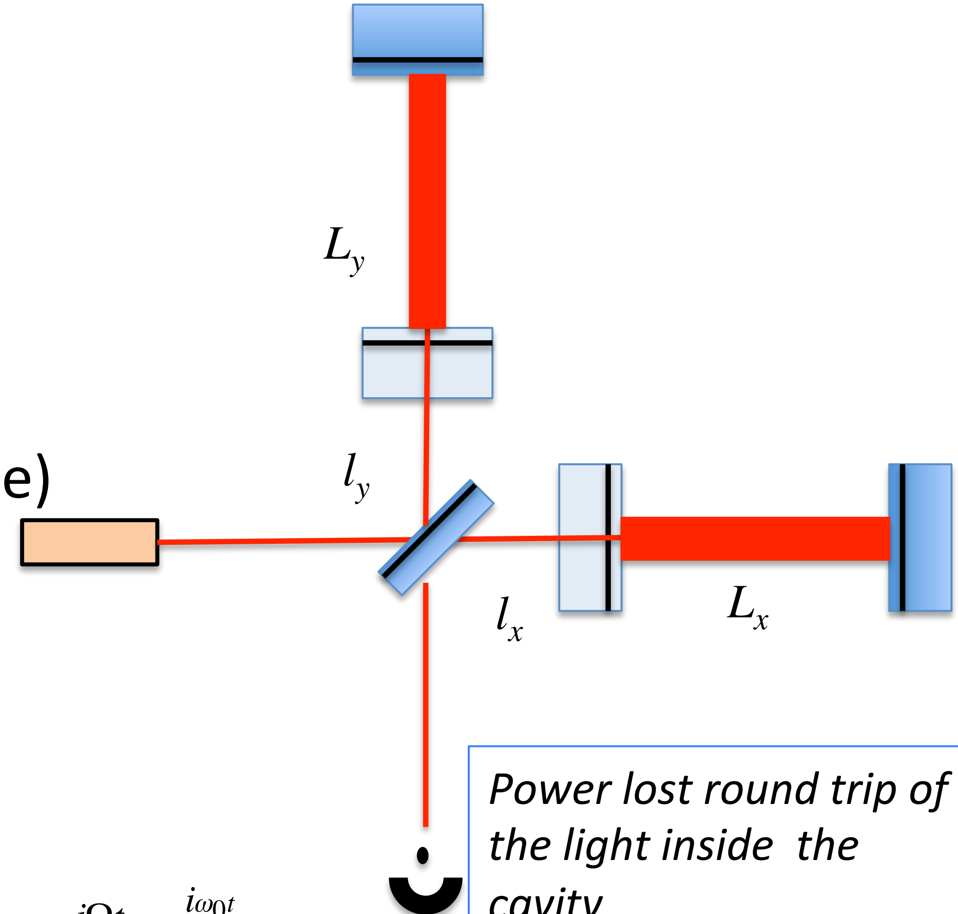

$$\Psi^{m}_{out}(t) = [A_c^{'}\Psi_0 + A_+^{'}\Psi_+ e^{i\Omega t} + A_-^{'}\Psi_- e^{-i\Omega t}]e^{i\omega_0 t}$$

Power lost round trip of the light inside the cavity

$$P_{out} = 2P_{in}J_oJ_1\frac{F}{\pi}\frac{\omega_o}{c}L\,h\sin\left(\frac{\Omega}{c}\Delta l_{Sc}\right)\bullet\left(1-\varepsilon\frac{F}{\pi}\right)$$

Michelson+ Fabry-Perot +Recycling

Power Recycling cavity (I)

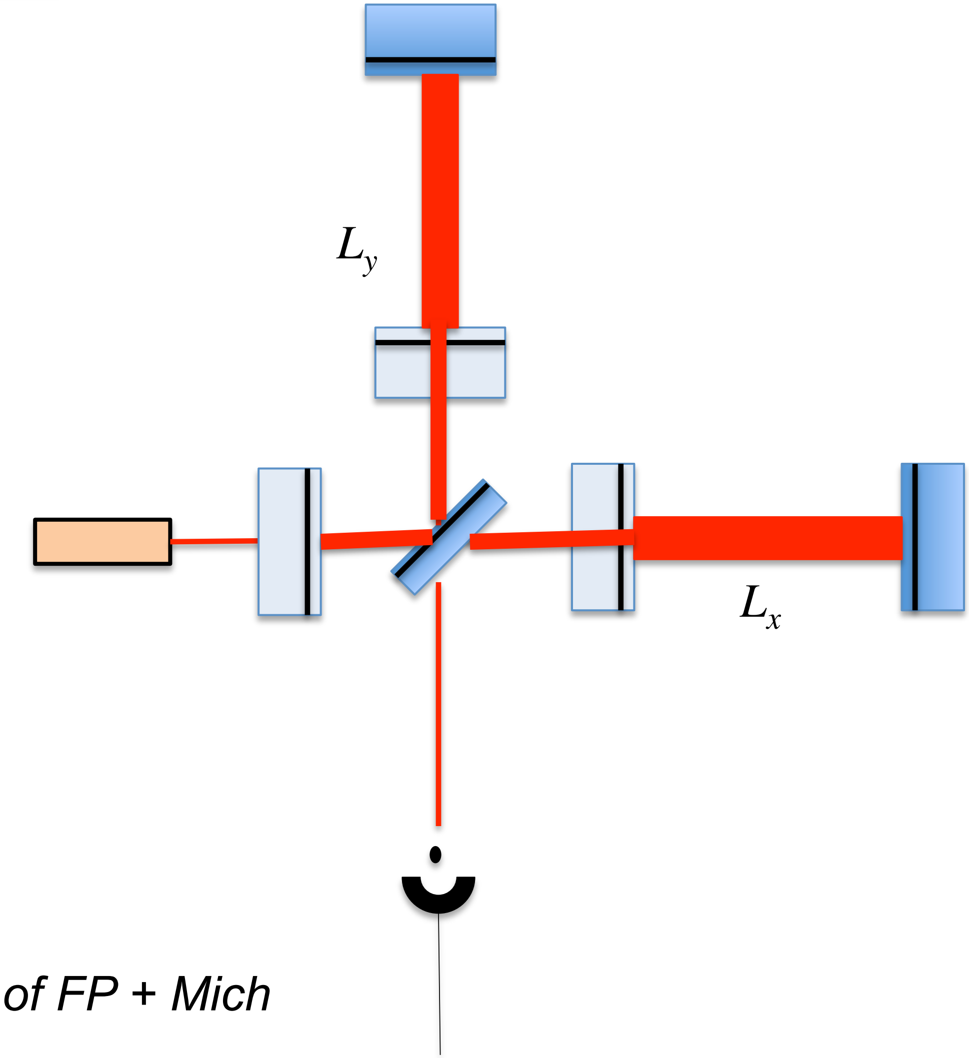

The most of the carrier gets reflected back towards the laser

Including the recycling mirrors means to add an other FP cavity

Transmission and reflection coefficients of the interferometer, including power recycling, are those of the cavity with the recycling mirror and the rest of the interferometer acting as the output mirror.

$$t_{rc} = \frac{t_{rm} t_{ifo} e^{i\frac{\omega_o}{c} l_{rc}}}{1 - r_{rm} r_{ifo} e^{i\frac{\omega_o}{c} l_{rc}}}$$

t_{ifo} and r_{ifo} ➔ *transmission and reflection of FP + Mich*

We separate the contribution of carrier and sidebands

$$\Psi_{out}^{m}(t) = [A''_c \Psi_0 + A''_+ \Psi_+ e^{i\Omega t} + A''_- \Psi_- e^{-i\Omega t}] e^{i\omega_0 t}$$

Power Recycling (II) -Sidebands

$$r_{\pm}^{ifo} = -e^{\pm i\frac{\Omega}{c}(l_x+l_y)} \cos(\frac{\Omega}{c}\Delta l_{Sc})$$

$$t_{\pm}^{ifo} = \mp e^{\pm i\frac{\Omega}{c}(l_x+l_y)} \sin(\frac{\Omega}{c}\Delta l_{Sc})$$

These relations, inserted in t_{ifo} and r_{ifo} bring to the conclusion that the resonance condition is

$$e^{i\frac{\Omega}{c}(2l_{rc}+l_x+l_y)} = -1$$

r

the optimum recycling is obtained for

$$r_{rm} = \cos(\frac{\Omega}{c}\Delta l_{Sc})$$

the transmission coefficients for the sidebands is

$$t_{\pm}^{ifo} = \pm i e^{\mp i\frac{\Omega}{c}l_{rc}}$$

Power Recycling (III) - Carrier

$$r_c^{ifo} = e^{i\frac{\omega_o}{c}(l_x+l_y)}(1-\frac{1}{\pi}F_{ac}\varepsilon)$$

$$t_c^{ifo} = ie^{i\frac{\omega_o}{c}(l_x+l_y)}2F\frac{L\omega_o}{\pi c}h(1-\frac{1}{\pi}F_{ac}\varepsilon)$$

In this case the resonance condition is

$$e^{i\frac{\omega_o}{c}(2l_{rc}+l_x+l_y)} = 1$$

the optimum coupling for the recycling is obtained for

$$r_{rm} = (1-\frac{1}{\pi}F_{ac}\varepsilon)$$

$$t_c^{rc} = ie^{-i\frac{\omega_o}{c}l_{rc}}2\frac{F_{ac}}{\pi}\sqrt{\frac{F_{rc}}{\pi}}\frac{\omega_o}{c}Lh$$

with

$$F_{rc} \approx \frac{\pi}{t_i^2}$$

Summary: carrier + sidebands conditions

Recycling reflectivity

$$\cos(\frac{\Omega}{c}\Delta l_{Sc}) = r_{rm} = (1-\frac{1}{\pi}F_{ac}\varepsilon)$$

Resonance conditions

$$e^{i\frac{\omega_o}{c}(2l_{rc}+l_x+l_y)} = 1$$

$$e^{i\frac{\Omega}{c}(2l_{rc}+l_x+l_y)} = -1$$

Signal Recycling

SR mirror reflects back into ITF adding coherently with more signal due to GW.
In practice we store the signal storage making more efficient the transfer of power from carrier to sidebands

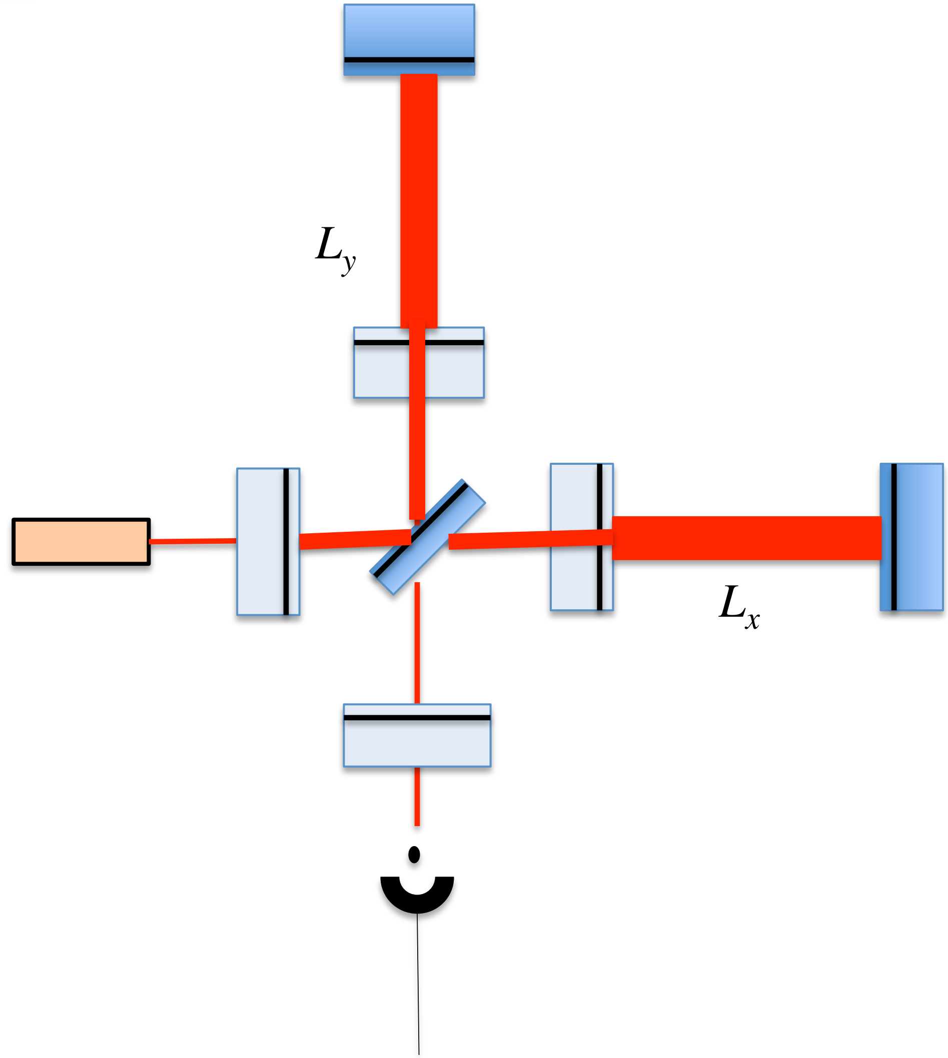

Two possible configuration:

Tuned ➔SR cavity resonates at ω_o

Untuned ➔SR cavity does not resonate at ω_o

Signal recycling (II)

- The signal sidebands will be sent back into the interferometer and
  - they can be coherently enhanced

  or
  - used to coherently extract more sideband amplitude from the arm cavities.

  In the later case, the ***SR mirror is placed at a position where the carrier is resonant in the SR cavity which increases the effective transmissivity of the ITMs***. The subsequent reduction in the finesse increases the bandwidth of the entire detector. This is called resonant sideband extraction.

- Changing the position of the SRM will increase the peak displacement sensitivity in a position dependent specific frequency range but will also reduce the bandwidth of the detector. This is commonly known as ***detuned signal recycling or detuned resonant sideband extraction.***

Signal Detection

Static output

$$P_{out} = 2P_{in} J_o J_1 \frac{F_{ac}}{\pi} \sqrt{\frac{F_{rc}}{\pi}} \; \frac{\omega_o}{c} Lh$$

As we have shown before, the finite storage time of the arm cavities introduces a single pole in the response of the interferometer with a cut-off frequency

$$f_o = c / 4L\, F_{ac}$$

Spectral output

$$P_{out}(f) = 2P_{in} J_o J_1 \frac{F_{ac}}{\pi} \sqrt{\frac{F_{rc}}{\pi}} \; \frac{\omega_o}{c} L \sqrt{\frac{f_o^2}{f_o^2 + f^2}} \; h(f)$$

Readout schemes

RF sidebands are modulated onto the light at the input of the Michelson and the out is demodulated via mixer driven by the RF signal

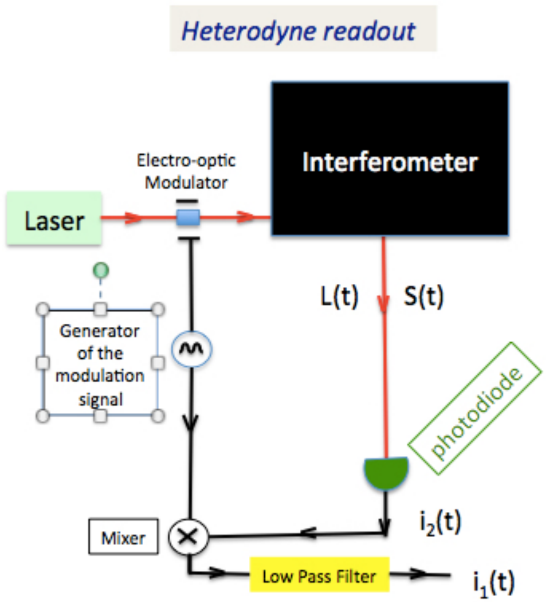

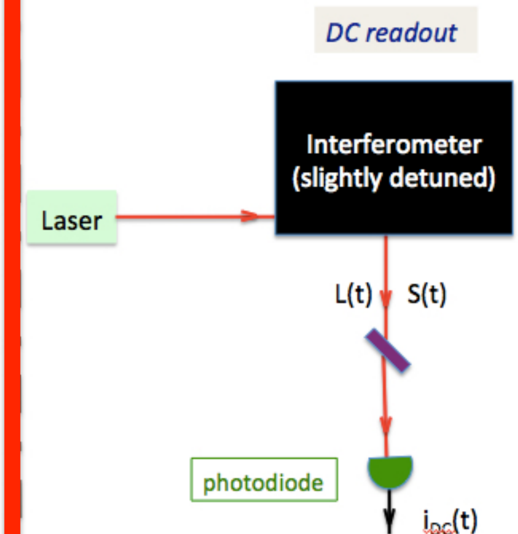

The local oscillator is the fraction of the carrier light that leaks into the signal port due to the residual interferometer asymmetry of the arms.

- Advantage: the DC detection to the respect of the heterodyne readout: the shot noise contribution from frequencies twice the heterodyne frequency does not exist
- Disadvantage: an increased coupling of laser power noise

$$S_{hom}(\Omega) = \frac{h^2}{2K}\frac{1}{t_{rc}^2}\frac{1}{\left|D_1 \sin\phi_{hom} + D_1 \cos\phi_{hom}\right|^2} \bullet$$
$$\bullet\{[(C_{11}\sin\phi_{hom} + C_{21}\cos\phi_{hom})^2 + (C_{21}\sin\phi_{hom} + C_{22}\cos\phi_{hom})^2] +$$
$$+[\frac{|D_+|^2 + |D_-|^2}{\left|D_+ e^{-i\phi_{dem}} + D_- e^{-i\phi_{dem}}\right|^2}]\}$$

2 Ω terms

$$S_{hom}(\Omega) = \frac{h^2}{2K}\frac{1}{t_{rc}^2}\frac{1}{\left|D_1 \sin\phi_{hom} + D_1 \cos\phi_{hom}\right|^2} \bullet$$
$$\bullet[(C_{11}\sin\phi_{hom} + C_{21}\cos\phi_{hom})^2 + (C_{21}\sin\phi_{hom} + C_{22}\cos\phi_{hom})^2]$$

Interferometer Control

ITF control: a complex problem

- **Coherent** *(Global Control)*: the operation point has to be locked by using ITF light. Angular control performed coherenty with respect to the light into the ITF by means of beam wavefront sensing (i.e. detection of $TEM_{01,10}$ modes due to misalignment

  ➔ relative position of mirrors is correlated by light

- **Incoherent** *(Local Control)* : the mirrors are controlled by means of independent ground-based sensors and quasi-inertial actuators.

  ➔relative position of mirrors is correlated by the ground

Global Control

Lock Requirements

Power recycling Interferometer

Feedback control system acting on the mirrors without reintroducing noise in the detection band.

Four independent lengths have to be controlled

$l_{rec} = 2\, l_{rc} + l_x + l_y$ ➔ Power recycling cavity length

$\Delta l = l_x + l_y$ ➔ Asymmetry length to be on dark fringe

L_x ➔ Lenght of the first long arm

L_y ➔ Lenght of the second long arm

Typical lock accuracy to be achieved 10^{-12} m $_{rms}$

Signal recycling Interferometer

\+

$l_{sec} = 2\, l_{sr} + l_x + l_y$ ➔ Signal recycling cavity length

Lock strategy

In practice the control is based the following physical degrees of freedom

$L_x - L_y$ ➔ DARM

$(L_x + L_y)/2$ ➔ CARM

$l_x - l_y$ ➔ MICH

$l_{rec} = l_{rc} + (l_x + l_y)/2$ ➔ *PRLC*

$l_{sc} = l_{sr} + (l_x + l_y)/2$ ➔ *SRLC*

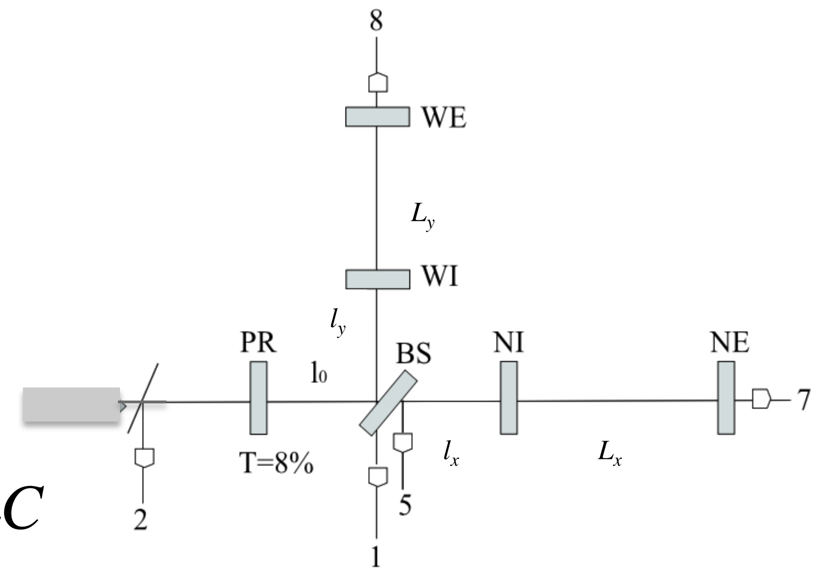

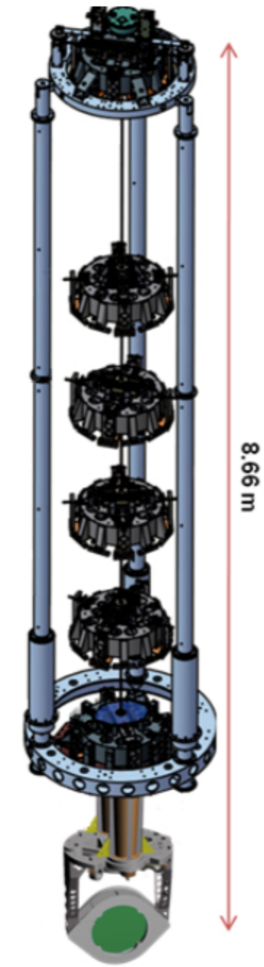

The mirror suspended swings ➔ Local control reduction➔ 1µm/s, then

Step 0 evaluate the residual
Step 1 actuate to reduce further the residual velocity
Step 2 feedback loop engaged

Driving Coefficients

B1 ➔ *DARM, the GW signal*
B2 ➔ *ITF Common mode*
B5 ➔ *central cavity*
B7 ≃ L_x
B8 ≃ L_y

Driving Matrix

Mirror/ DOF	DARM	CARM	MICH	PRCL	SRC
NE	-1/2	-1			
WE	1/2	-1			
BS			1/√2		
PR			-1/2	-1	
SR			1/2		-1

Basic interference setup: two conditions

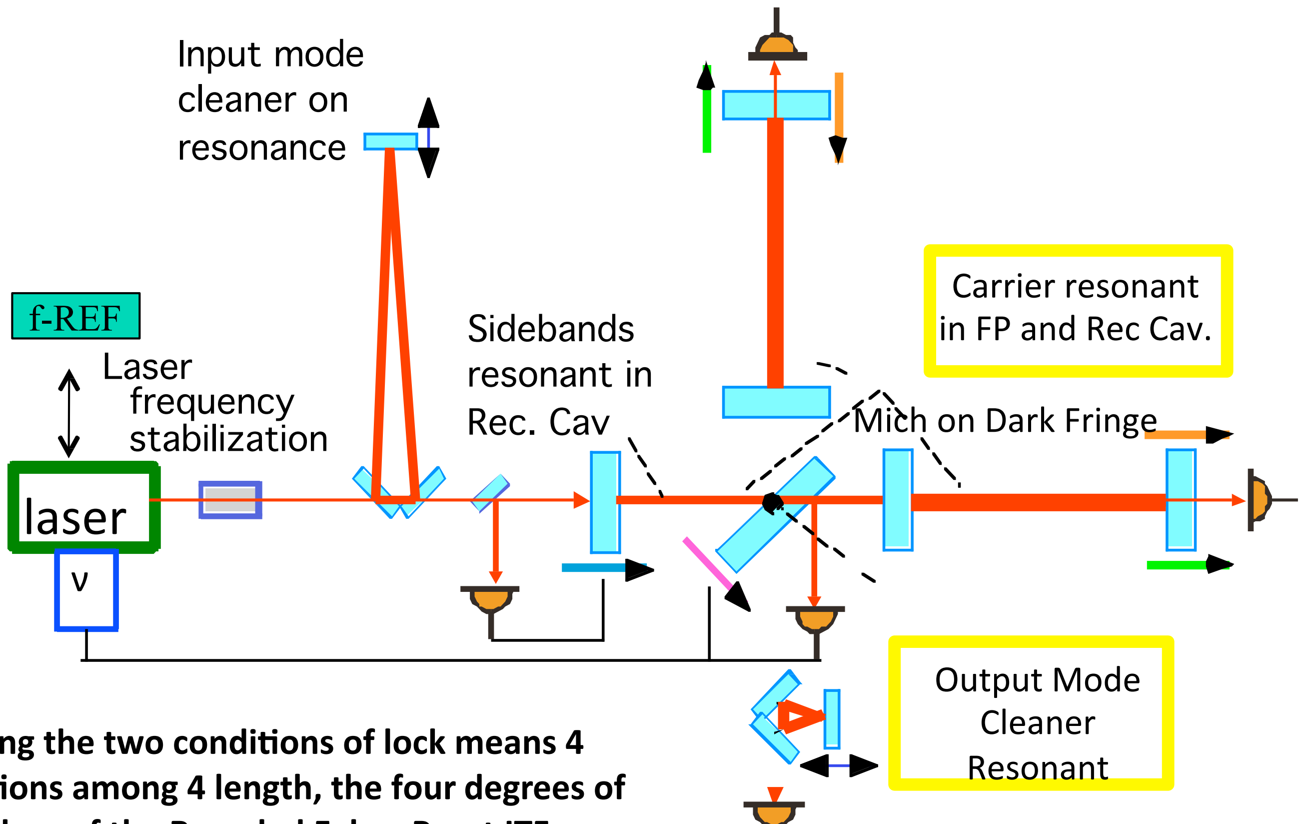

Setting the two conditions of lock means 4 relations among 4 length, the four degrees of freedom of the Recycled Fabry-Perot ITF

Dark Fringe set point (MICH)

Differential Arm length (DARM)

Power Recycling Cavity Length (PRCL)

Common Arm length (CARM)

Control noise vs. mirror actuation

- The force needed to acquire the lock is much larger than that needed to keep it. We need momentum to stop the mirror
- Drawback: "Strong actuation" means large electronic noise

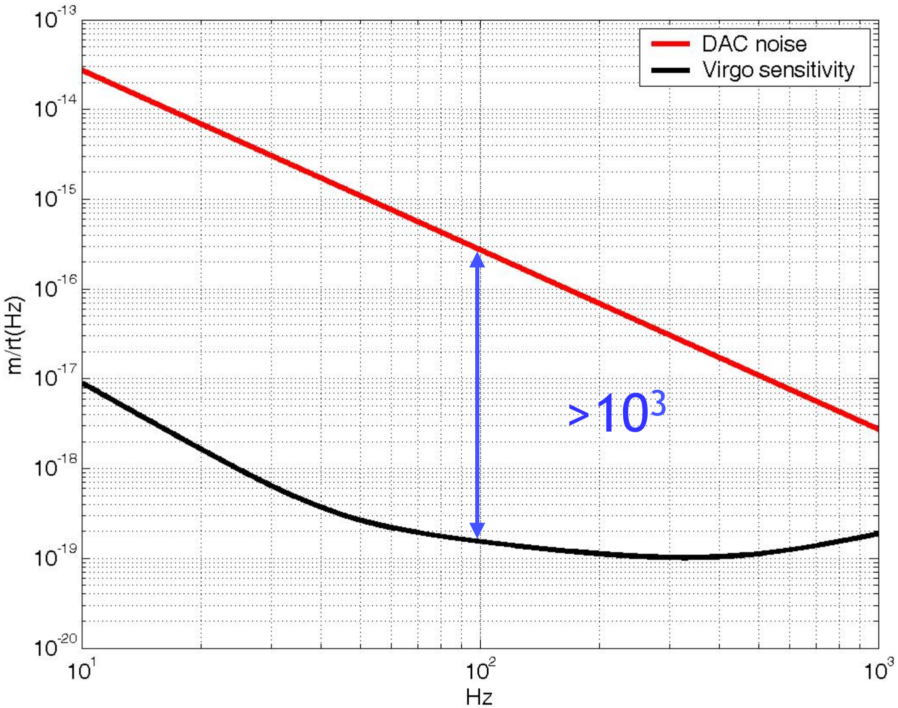

Velocity Limits

1) Response of the feedback loop	$v_{max1} = \pi\lambda B / F$ with B=loop bandwidth
2) Maximum available force F_{max}	$v_{max2} = (\lambda F_{max} / 2mF)^{1/2}$
3) time to cross resonance > light storage time	$v_{max3} = \pi\lambda c/(4 F^2 L)$ with B=loop bandwidth

Variable Finesse Method

Main peculiarity: the finesse of the recycling cavity changes during the lock acquisition sequence

Rational: operate with all the degrees of freedom are weakly coupled and independently controllable, making the control scheme much easier.

All four longitudinal degrees of freedom of the ITF are stably locked in a configuration that is easy to lock: a recycled ITF with a very low recycling gain

Step (a): locking it on the half fringe, so that a large fraction of light escapes through the antisymmetric port and the power build-up inside the recycling cavity is extremely low.

Step (b): ITF adiabatically brought to the operating point with the Michelson on the dark fringe.

Increasing of the recycling gain

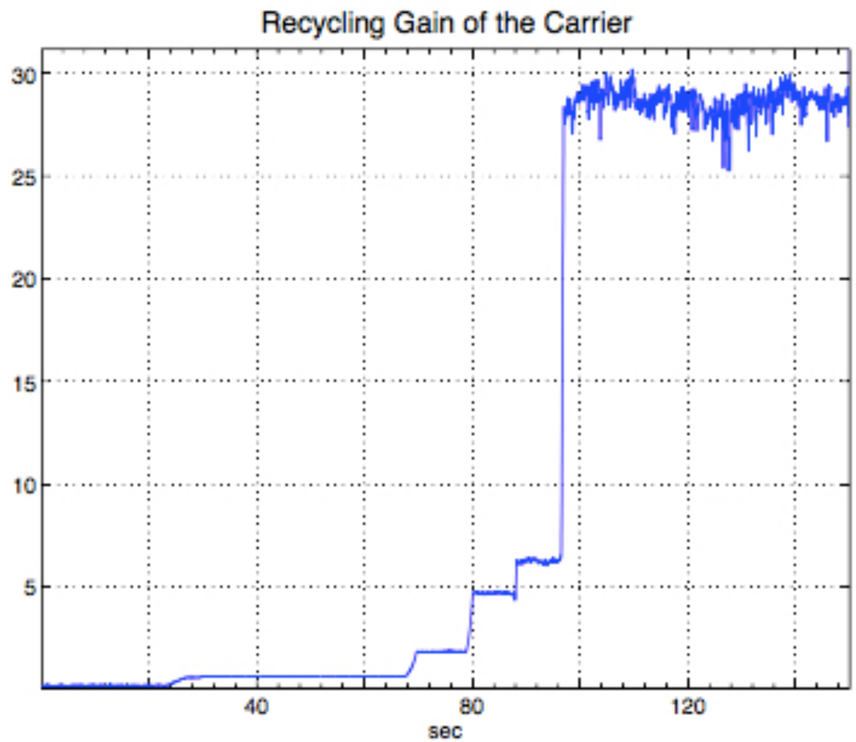

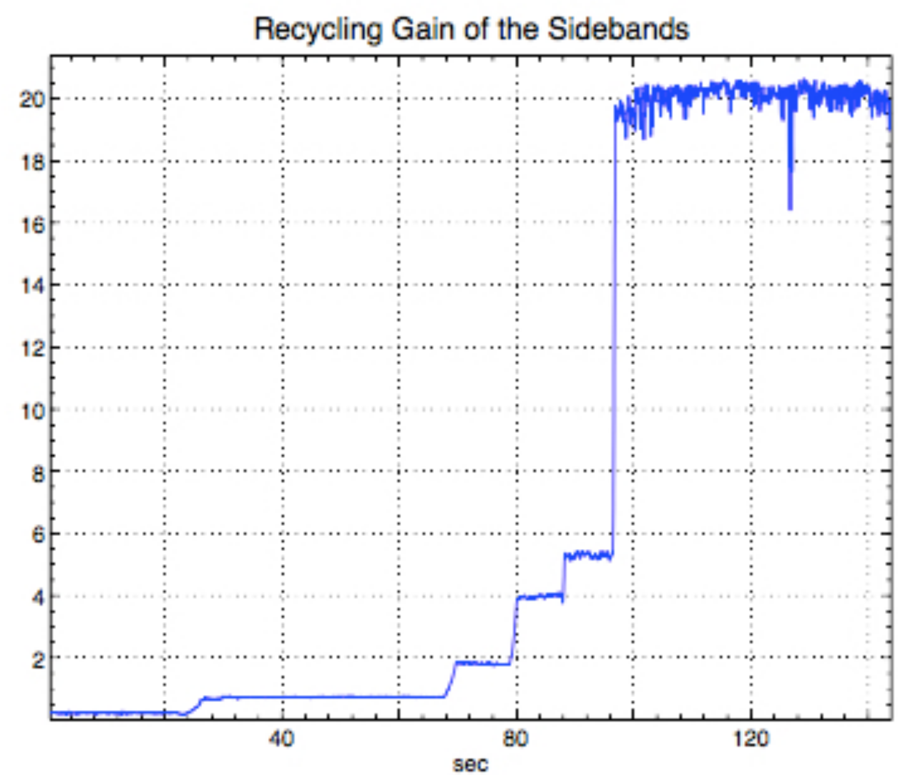

Local Control

The strategy

1) single point suspension, 2) DOF separation, 3) inertial damping, 4) hierarchical control (small forces close to the test mass)

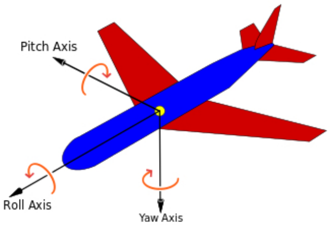

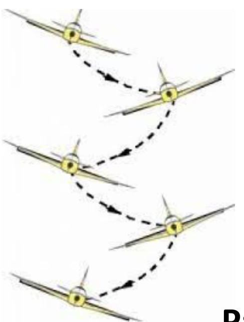

Yaw mode

	stage	variable	actuator ref
A	SA TOP	**Pos/Accel** 3D+yaw	Ground(~)/ fixed stars
	SA BOTTOM	**Position** 2D+yaw	Ground
Payload	MARIONETTE	**Position** 2D+pitch/yaw	SA BOTTOM
	MIRROR	**Position** 1D+pitch/yaw	Last Filter of SA

Basic requirements: sensing and actuation diagonalization

+

hiearchical control

Mirror suspension control

→ The Superattenuator is a multi-stage pendulum, with **passive attenuation**:

$$S^{1/2}(f) \approx \frac{10^{-7}}{f^2} m/\sqrt{Hz} \qquad (f > 1 \quad Hz)$$

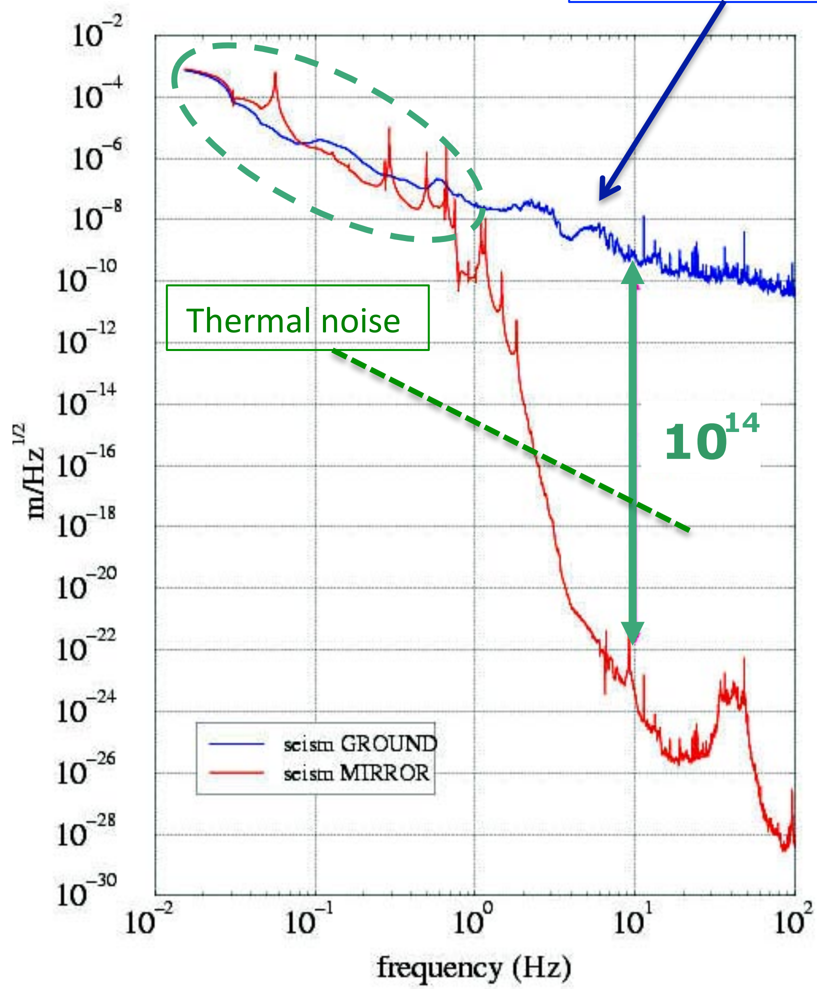

At lower frequencies the noise is instead totally transferred to the mirror, even amplified by the pendulum resonances

⇩

Local active control of the Superattenuator reduces mirror motion below a few Hz

⇩

Residual longitudinal motion of the mirror $\delta L \sim$ **10^{-6} m RMS**

Similar approach in TAMA, GEO and KAGRA

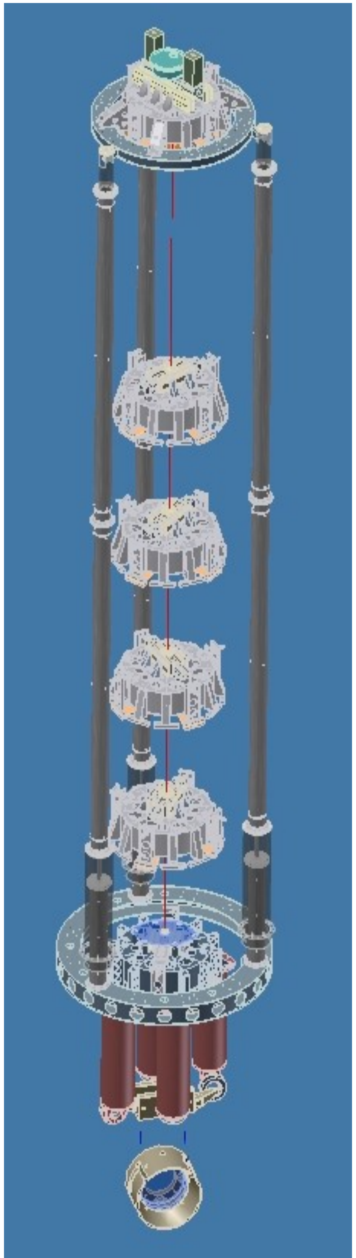

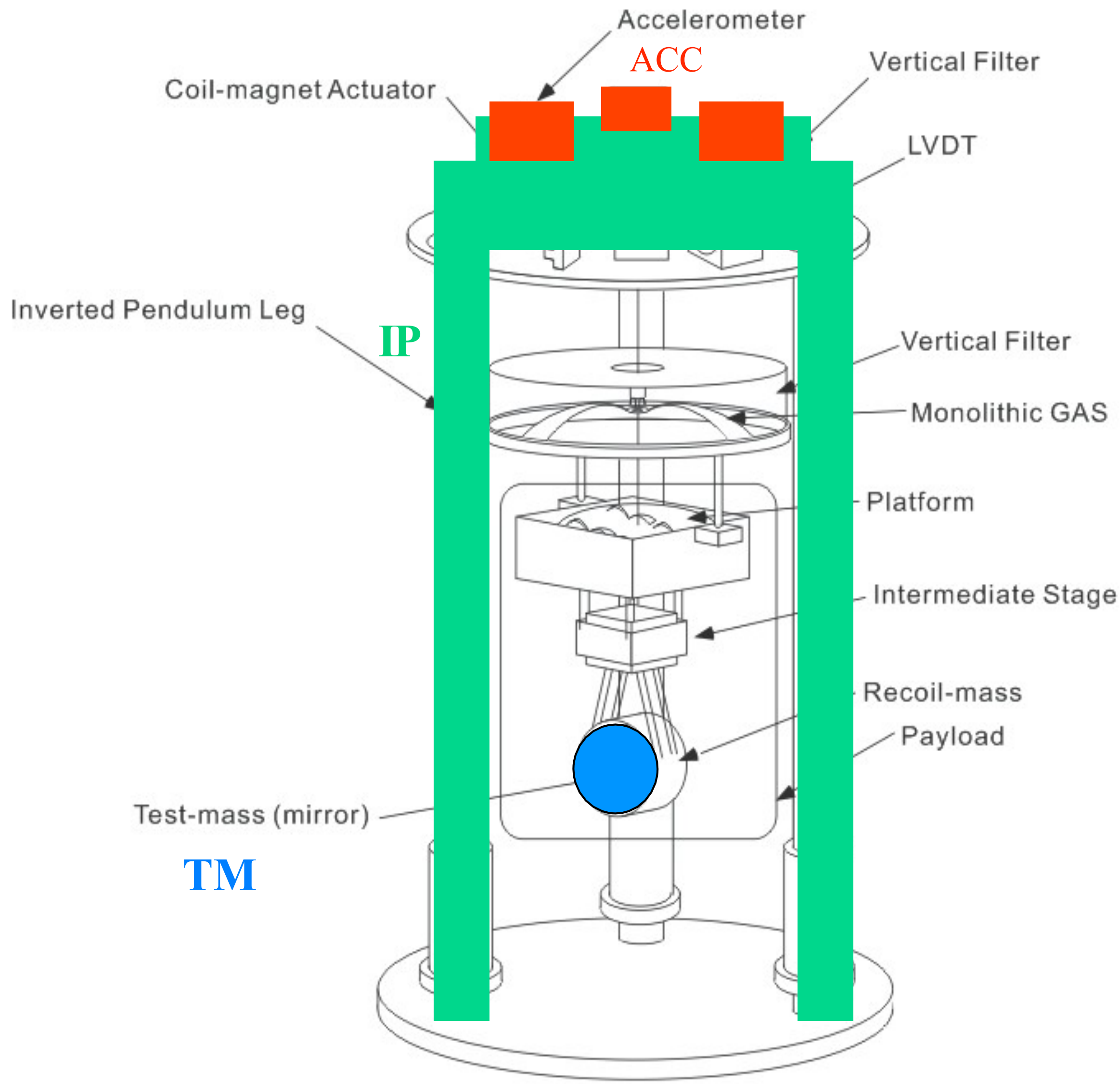

LIGO

Passive (to reduce noise in sensitive freq. band)

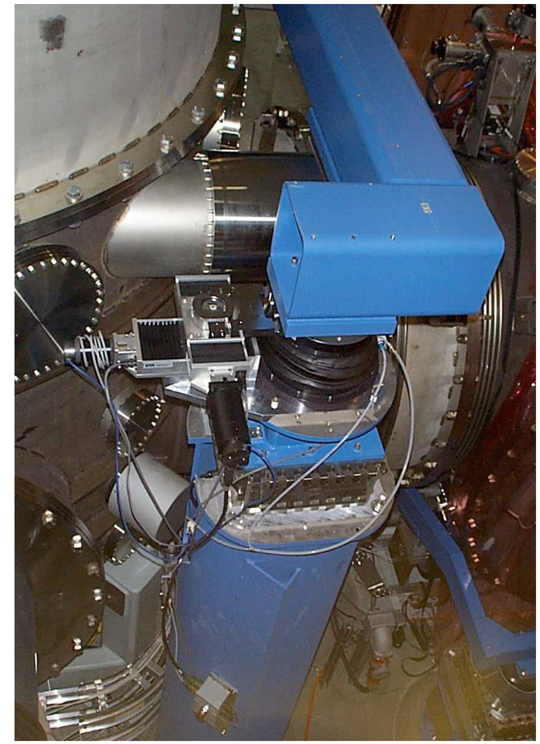

Active (to improve lock acquisition/maintenance)

AdV-LIGO seismic isolation: different approach based on active suppression

- One new approach is ‘active’ suppression, used in Advanced LIGO
  - Low-noise seismometers on payload detect motion in all six degrees-of-freedom
  - Actuators push on payload to eliminated perceived motion
  - Multiple 6-DOF stages to achieve desired suppression, allocation of control
- Challenges in structural resonances, sensor performance
- Nice to have a quiet table to mount lots of stuff on
- Enhanced LIGO using this approach for one chamber per interferometer
  - Meets requirements, will remain in place for AdvLIGO

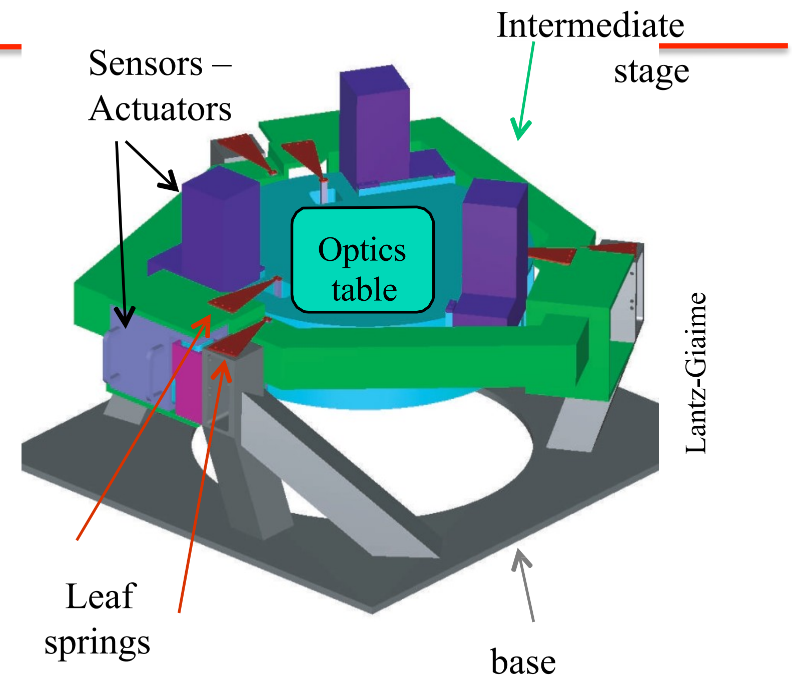

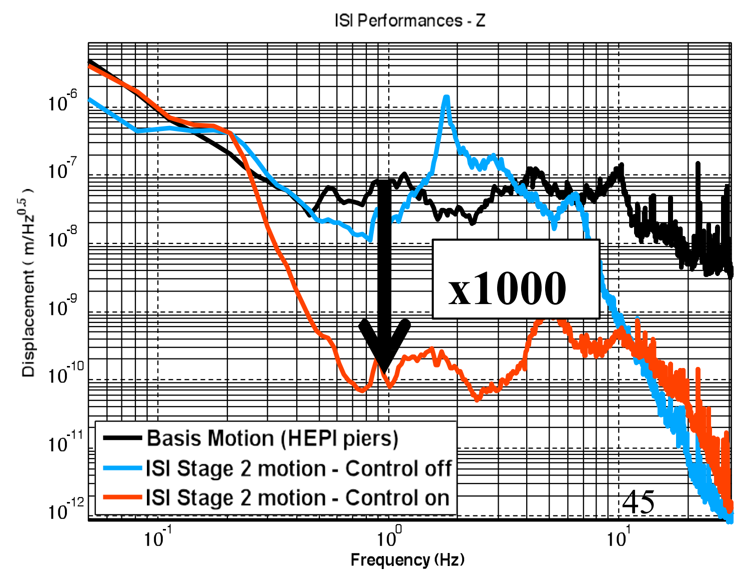

credits D. Shoemaker

Virgo Suspensions

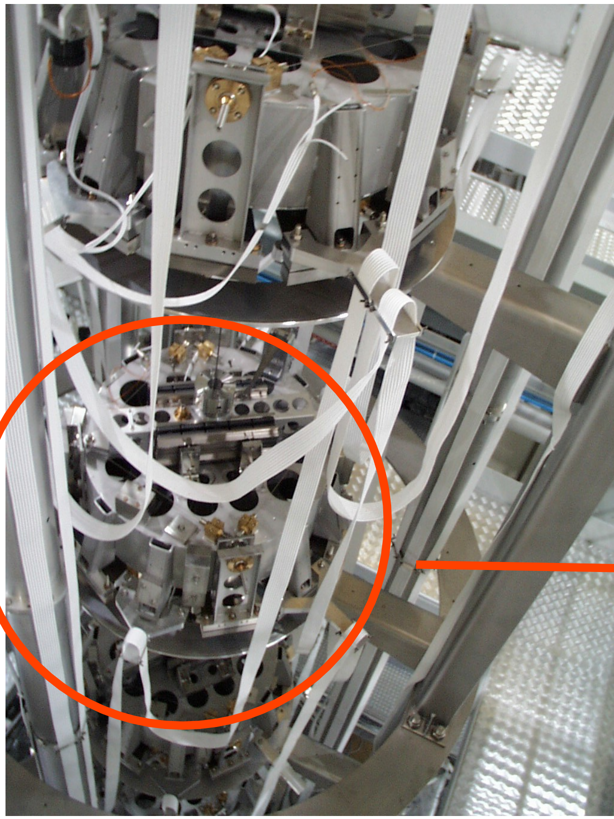

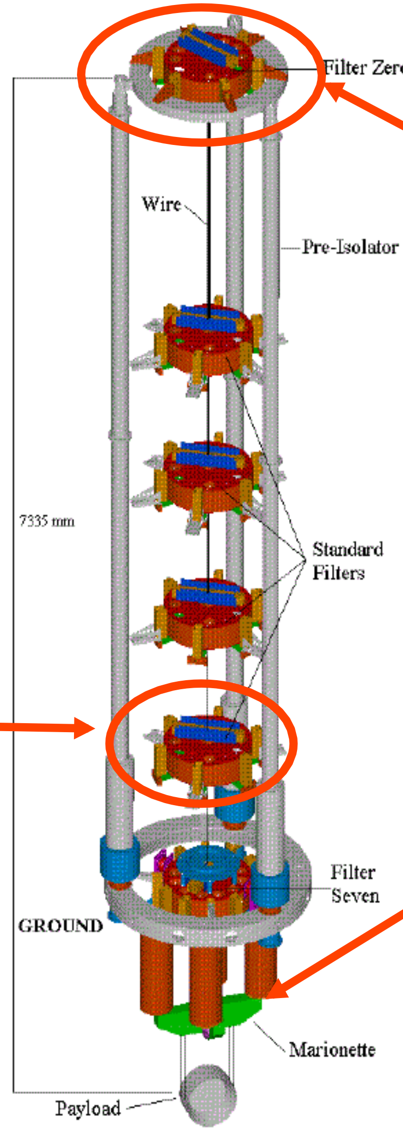

At 10 Hz seismic displacement is 10^{12} times larger than expected GW

Local Controls: Inertial Damping

- Inertial sensors (accelerometers):
  - DC-100 Hz bandwidth
  - Equivalent displacement sensitivity: 10^{-11} m/sqrt(Hz)
- Displacement sensors LVDT-like:
  - Used for DC-0.1 Hz control
  - Sensitivity: 10^{-8} m/sqrt(Hz)
  - Linear range: ± 2 cm
- Coil magnet actuators:
  - Linear range: ± 2 cm
  - 0.5 N for 1 cm displacement
- Loop unity gain frequency:
  - 5 Hz
- Sampling rate:
  -10 kHz

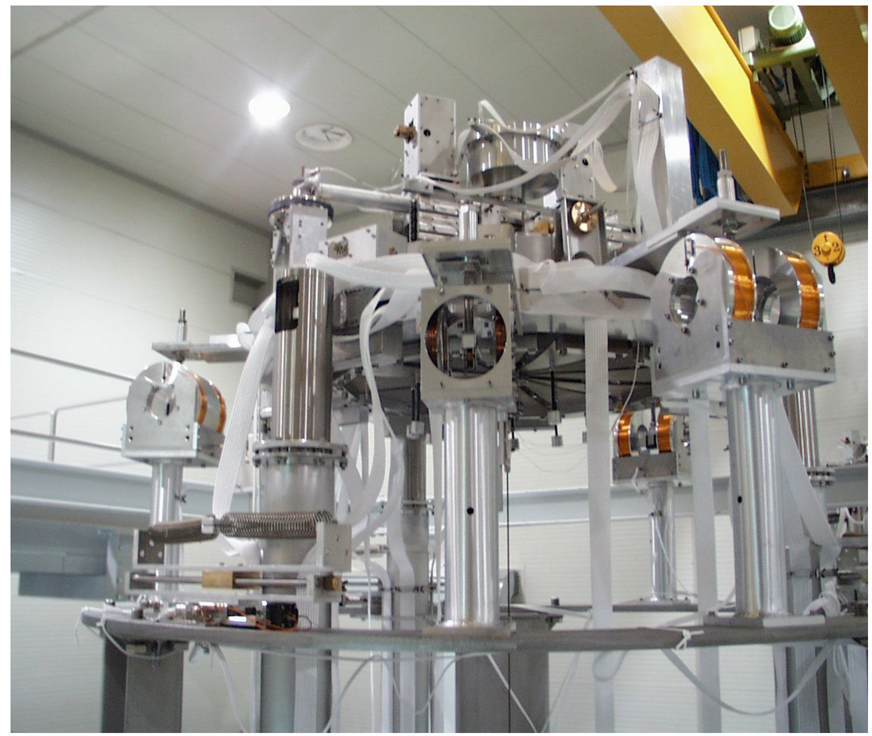

Achieving control

Soft isolator concept:

1. very efficient passive attenuation
2. active controls for suspension mode damping

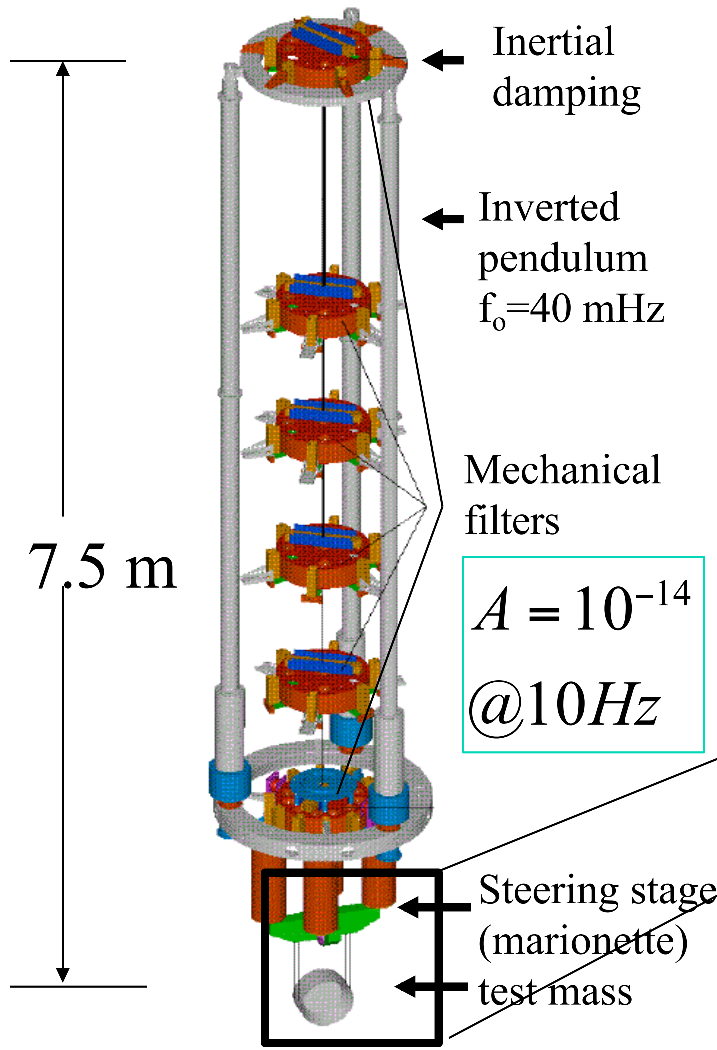

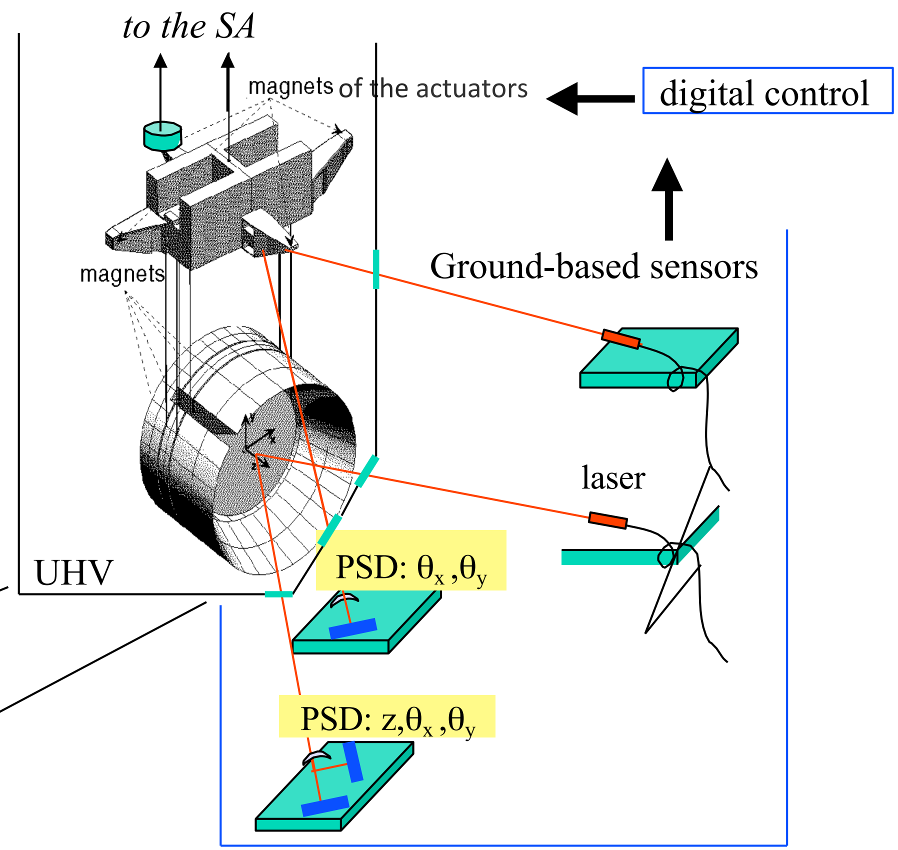

$\delta\theta_x = \delta\theta_y < 0.1$ μrad RMS, $\delta z = 0.5$ μm RMS

Drift (1 h) ~1 μrad

Range: 5×10^4-5×10^{-2} μrad, 10^4-0.1 μm

VIRGO

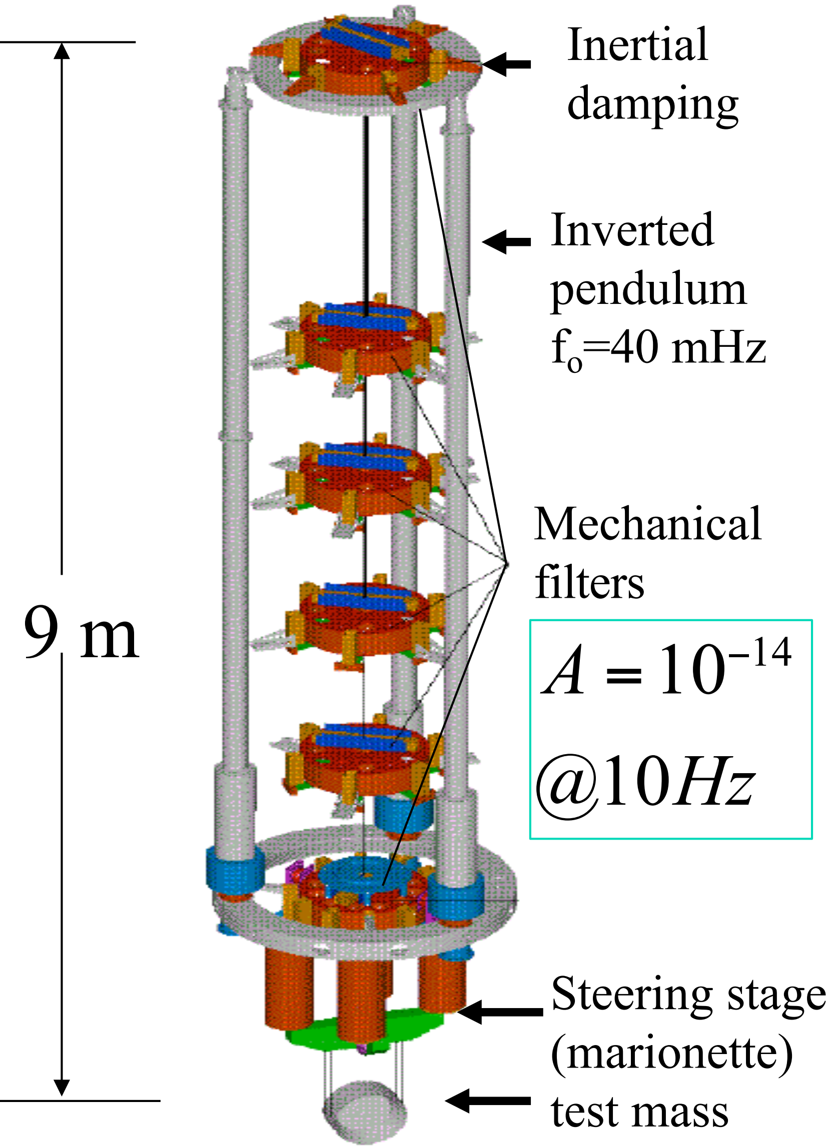

$$A = 10^{-14}$$
$$@10Hz$$

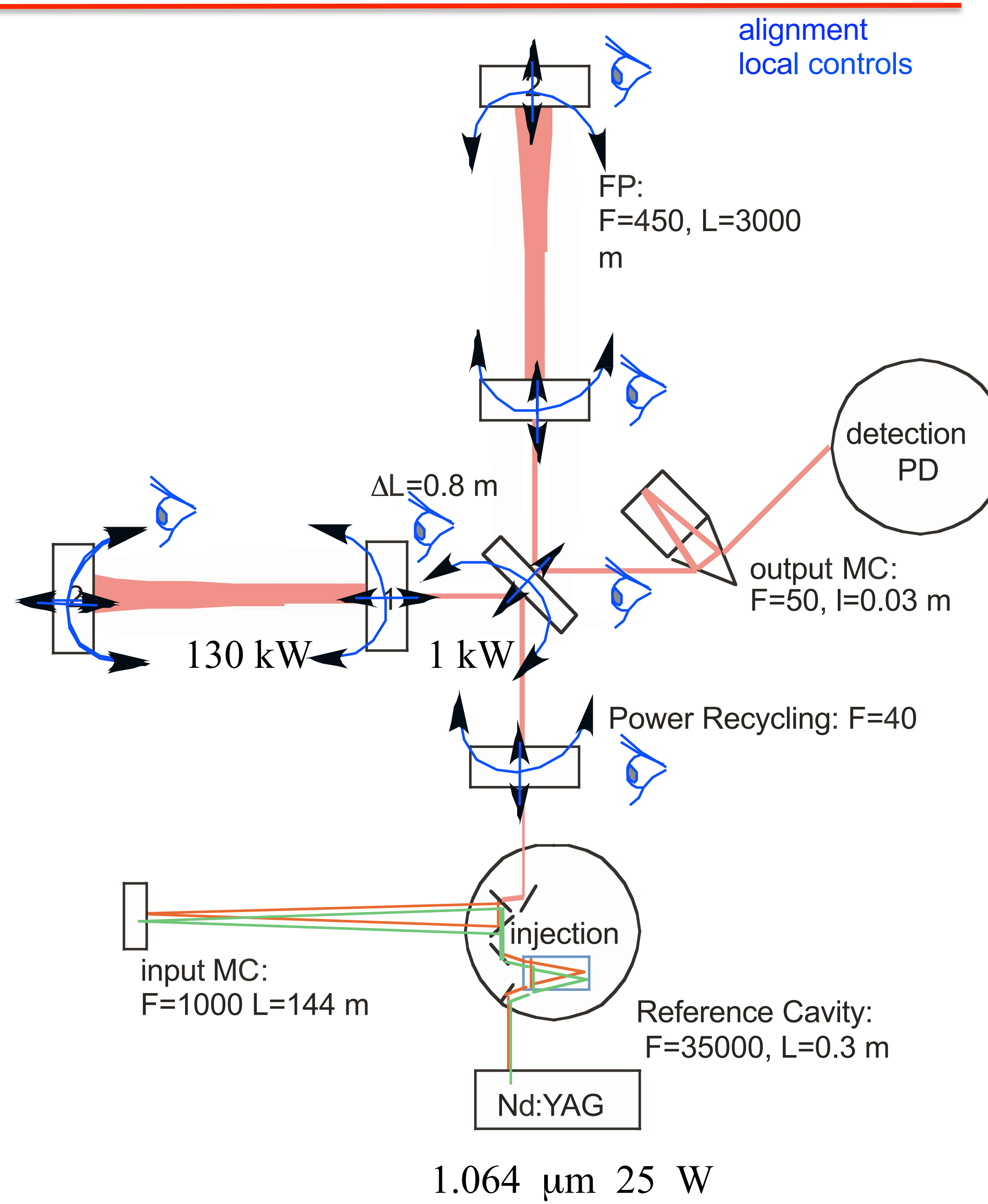

Optical levers

PSD device on the lens focal plane, *D= f*,
sensitive to mirror rotation

$$x_{PSD} = 2z\sin i\ (1-\frac{D}{f}) + 2\delta i\left[L(1-\frac{D}{f})\right]$$

PSD device on the lens image plane, *D= Lf/(L-f)*,
sensitive to mirror translation

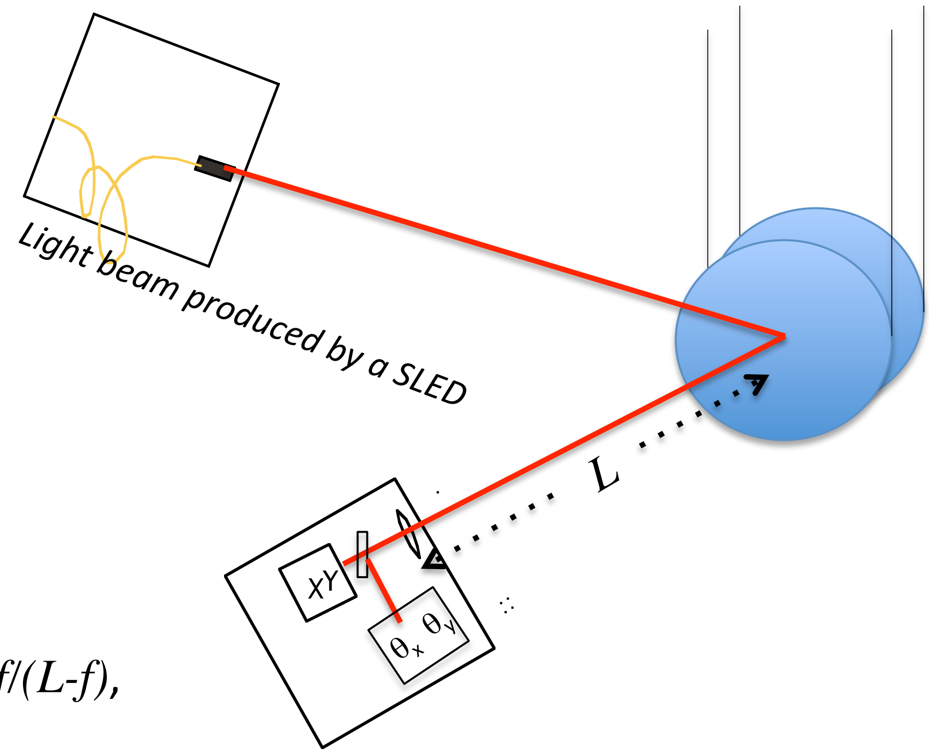

- Optical diagonalization of optical levers allow to reduce the coupling among mirror d.o.f. to <1%
- Large dynamics: 50 mrad < 80 nrad thanks to hybrid sensor system

Controls suspended actuators

I) Local controls apply corrections to mirror position using local sensors: swinging interference

II) Local controls receive error signals from global sensors. ITF Locked, resonant light

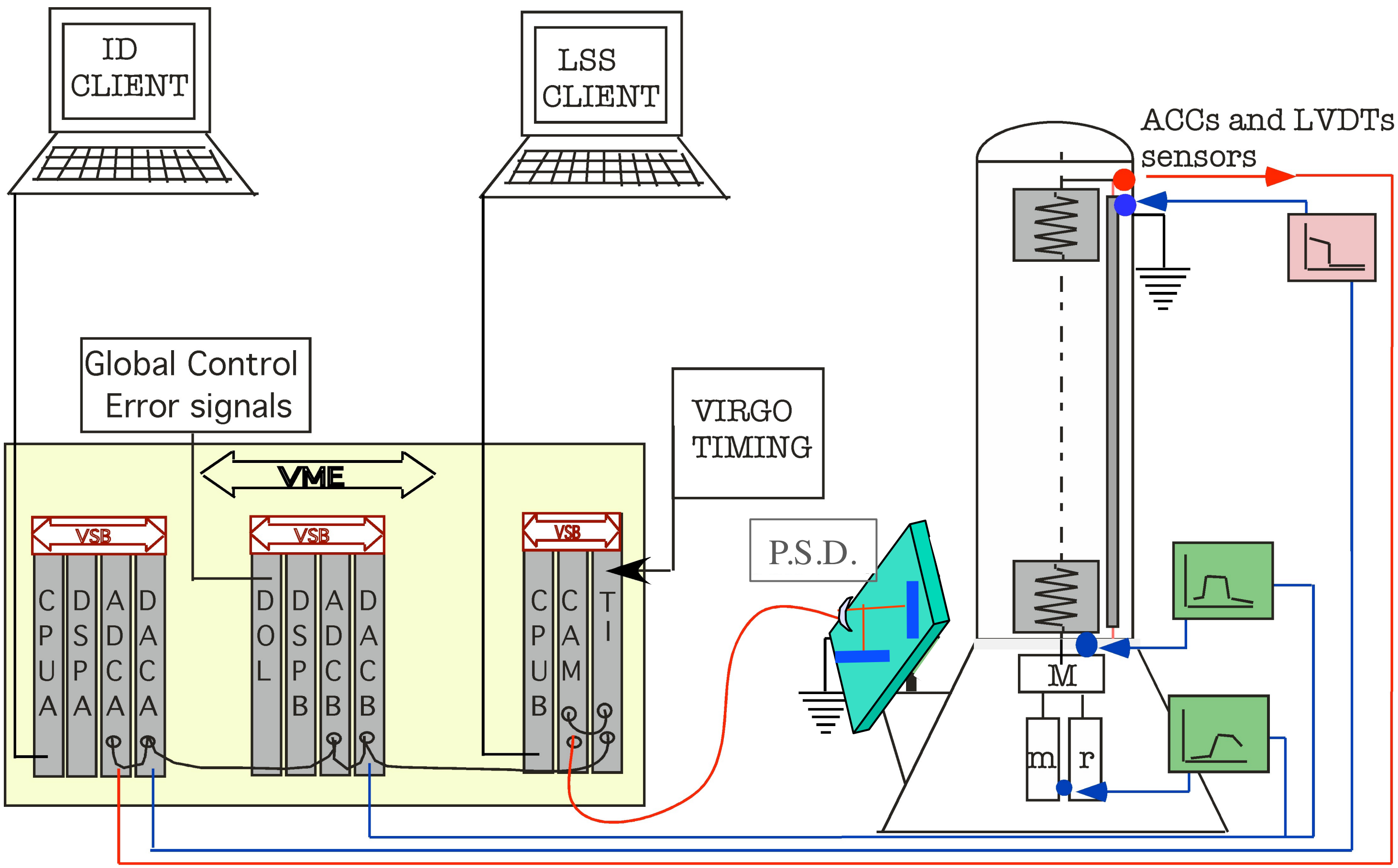

The sensitivity curve

Noise Formalism

$x_n(t)$ ➔ a stochastic variable with gaussian statistic and associated to a stationary process

For a stationary and ergodic process (statistical invariance to the respect of the time translation) the time dependence is limited to the time difference $\tau = t_1 - t_2$.

Auto correlation

$$R_{xx}(\tau) = E[x(t+\tau)x(t)] = \lim_{T\to\infty} \frac{1}{2T} \int_{-T}^{+T} x(t+\tau)x(t)dt$$

Properties

$$R_{xx}(0) = E[x^2(t)] = \eta^2 + \sigma^2$$

$$R_{xx}(0) \geq R_{xx}(\tau) \qquad \forall \quad \tau$$

$$R_{xx}(\tau) = R_{xx}(-\tau)$$

Sensitivity (I)

The amplitude of a GW is a strain, a dimensionless quantity h_s.
This gives a fractional change in length, or equivalently light travel time, across a detector.

The detector sensitivity is a measure of the capability to extract the signal h_s from the detector noise

This is usually done by optimizing the Signal to Noise Ratio (SNR) by the matched filter (Wiener filter in the case of δ signal),

$$SNR = \rho^2 = \int_{-\infty}^{+\infty} d(f) \frac{H_s^2(f)}{S_n(f)}$$

$H_s(f)$ ➔ Fourier transform of h_s with dimensions $(Hz)^{-1}$

$$H_s(f) = \int_{-\infty}^{+\infty} h_s(t) \exp(-i2\pi f\, t)\, dt \qquad S_n(f) = \int_{-\infty}^{+\infty} R_{hh}^{(n)}(\tau) \exp(-i2\pi f \tau)\, d\tau$$

Sensitivity (II)

$$h_{rss}^2 = \int [|h_+(t)|^2 + |h_x(t)|^2] dt$$

For a linearly polarized GW, with $H(f)$ constant across the bandwidth Δf

$$h_{rss} \simeq H(f) \ (\Delta f)^{1/2}$$

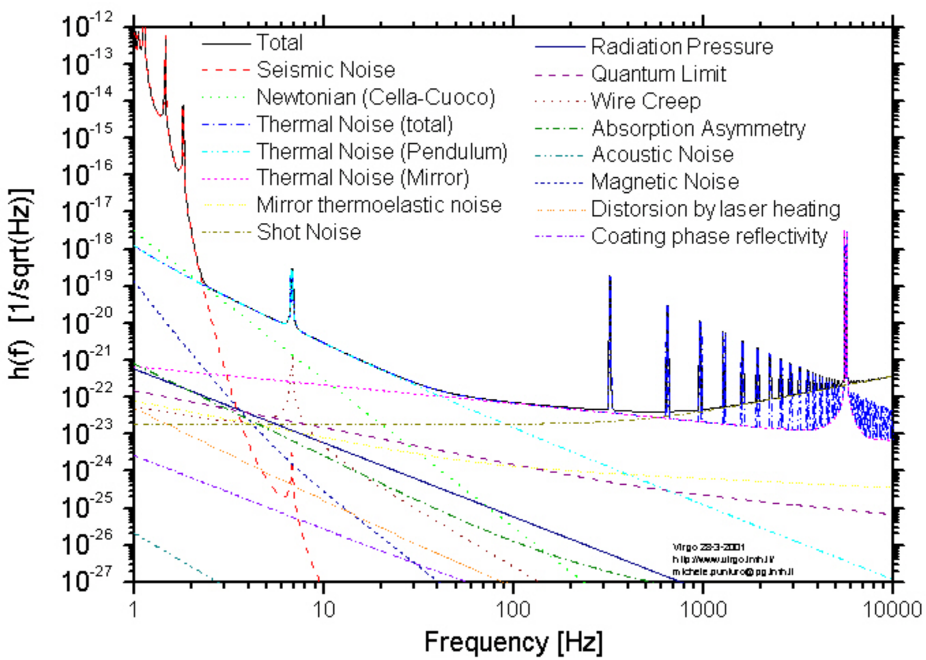

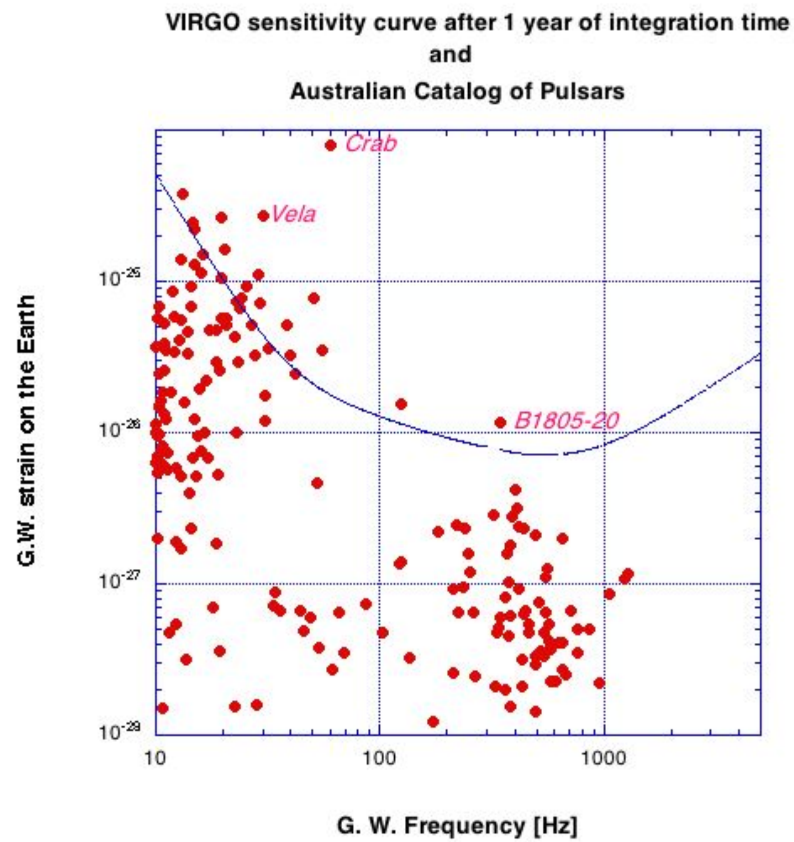

The detector

Implementation overview: vacuum system

- Requirements:
  - 10^{-9} mbar for H_2
  - 10^{-14} mbar for hydrocarbons
- Status:
  - Whole tube welded, leak-tested and baked and evacuated
  - 160 steel baffles for reflected light shielding installed
  - Vacuum performance within requirements

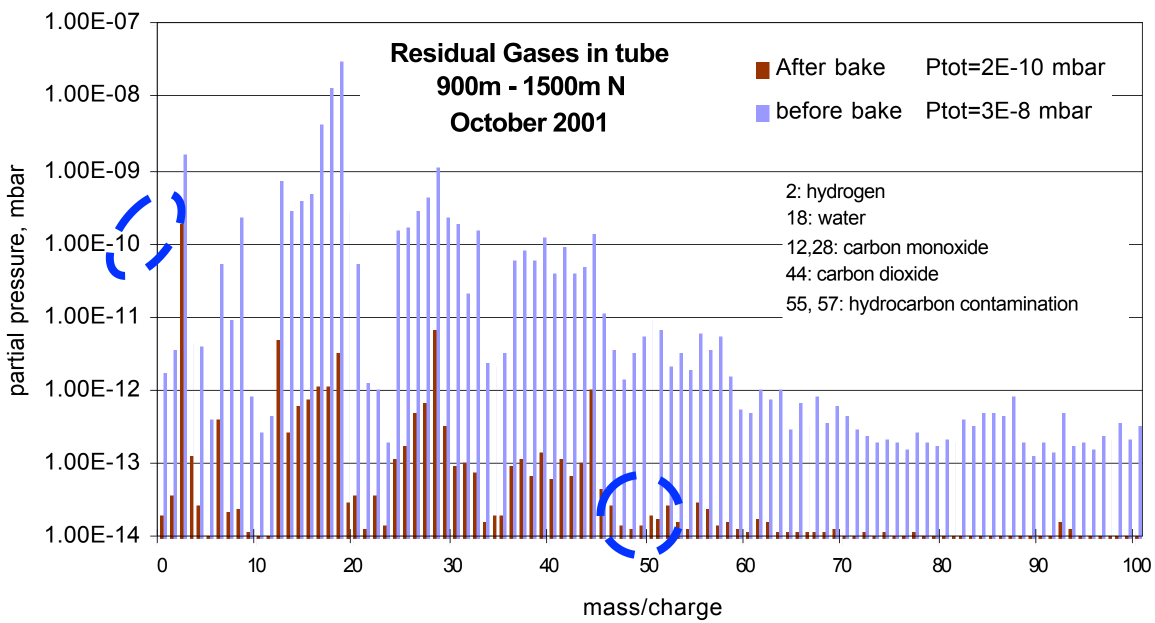

Implementation overview: mirrors

- High quality fused silica mirrors
  - 35 cm diameter, 20 cm thickness
  - Substrate losses: ~ 1 ppm
  - Coating losses: <5 ppm
  - Surface deformation: $\lambda/100$ (rms on 150mm)
  - ΔR: $<10^{-4}$

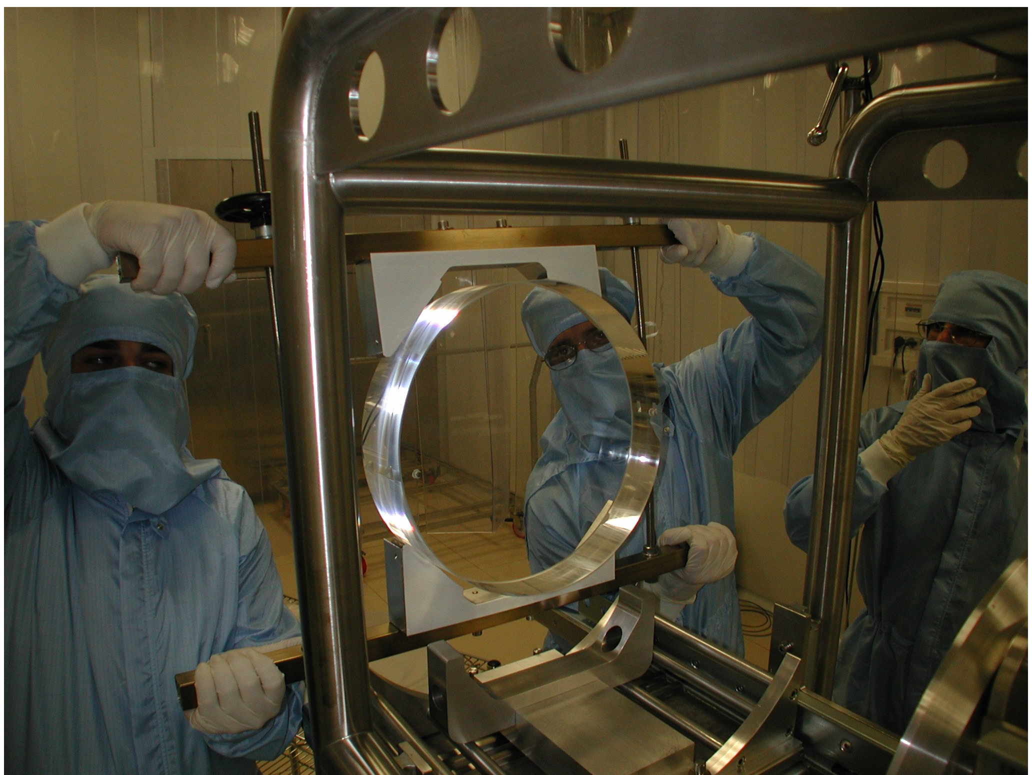

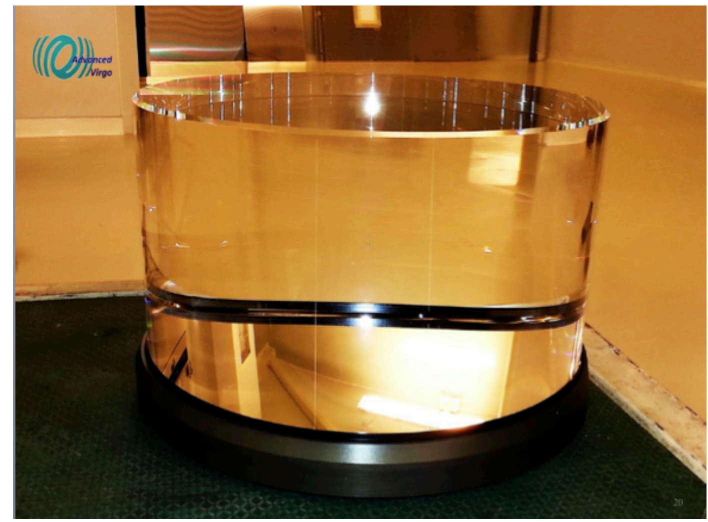

IPN - Lyon

Implementation overview: laser

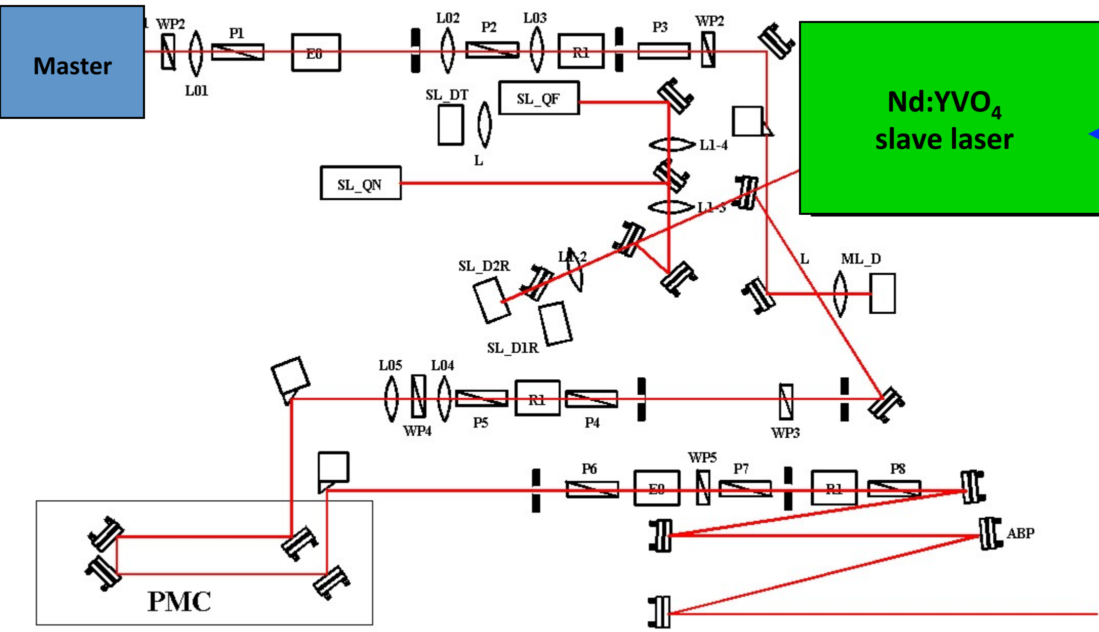

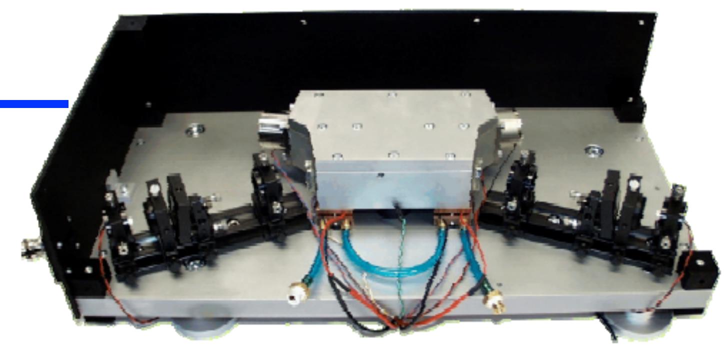

•Nd:YAG master commercial CW single mode (700 mW) @1064 nm

•Phase locked to a Nd:YVO$_4$ slave (monolithic ring cavity)

•Pumped by two laser diodes at 806 nm (40 W power)

•Output power: 25 W

Implementation overview: injection SYS

- Laser frequency locked to the Input Mode cleaner
- Input Mode Cleaner length locked to the reference cavity (monolithic)
- Final stage: ITF common mode as frequency reference

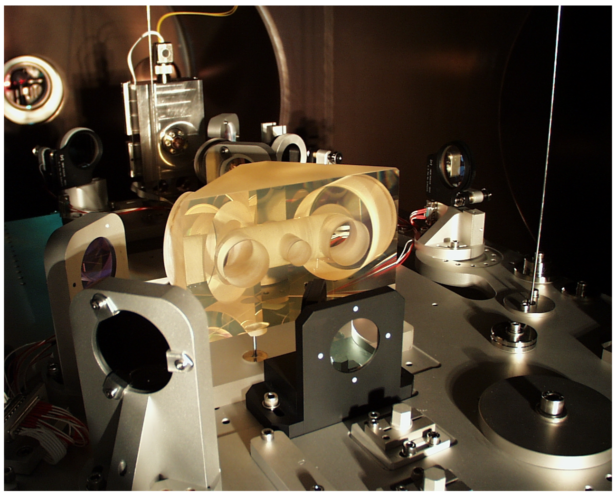

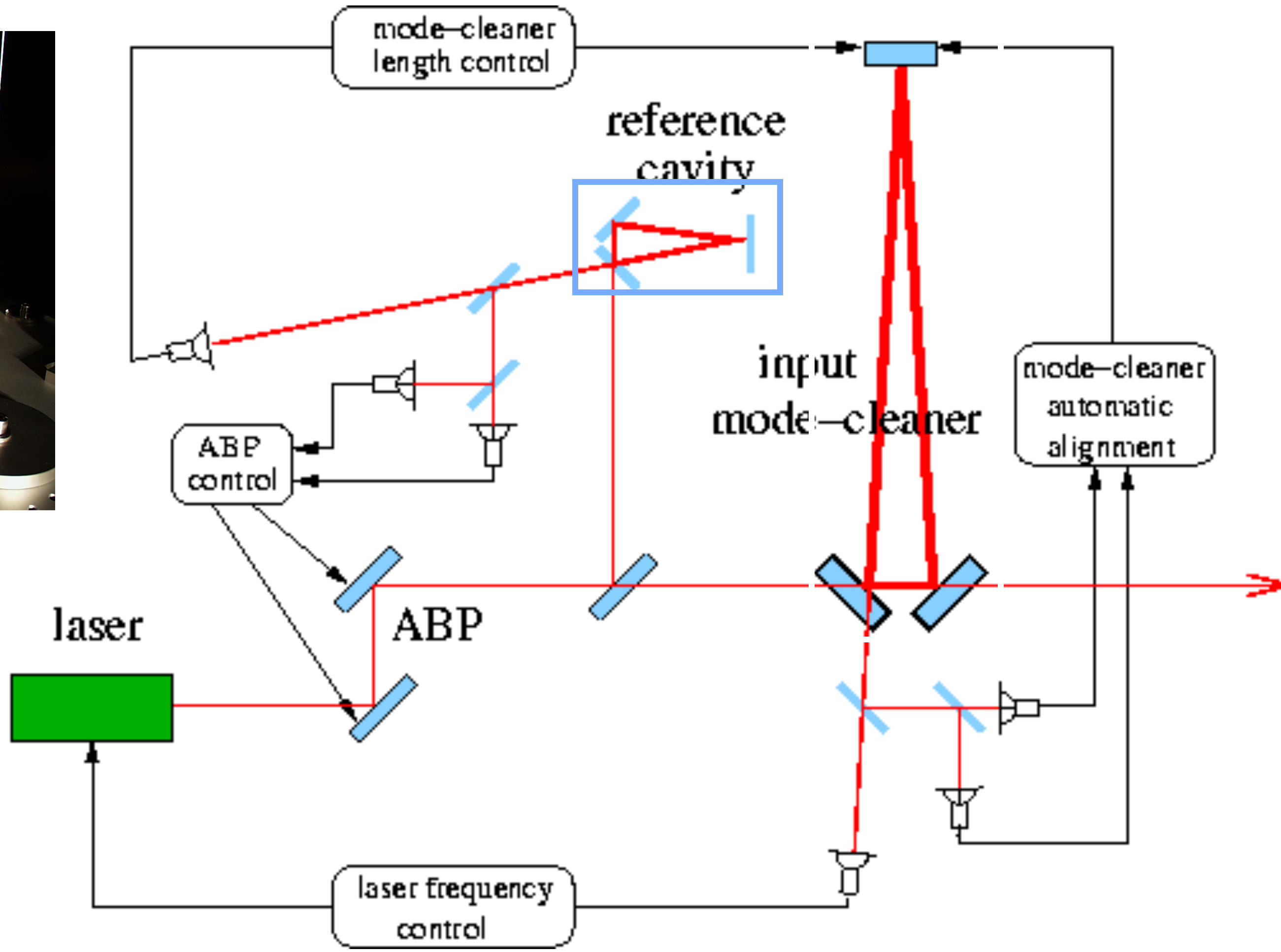

Frequency stabilization requirements: up to 10^{-4} Hz/√Hz at 1 Hz

Detection SYS: the old approach

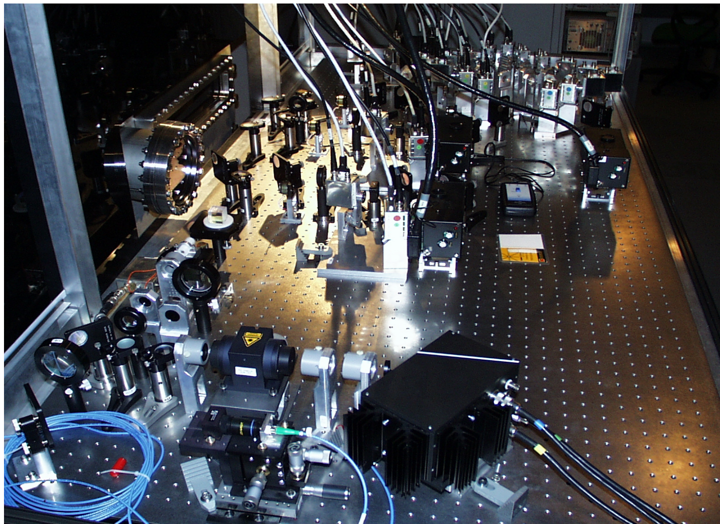

- In-vacuum output mode cleaner (spatial filtering of fake light)

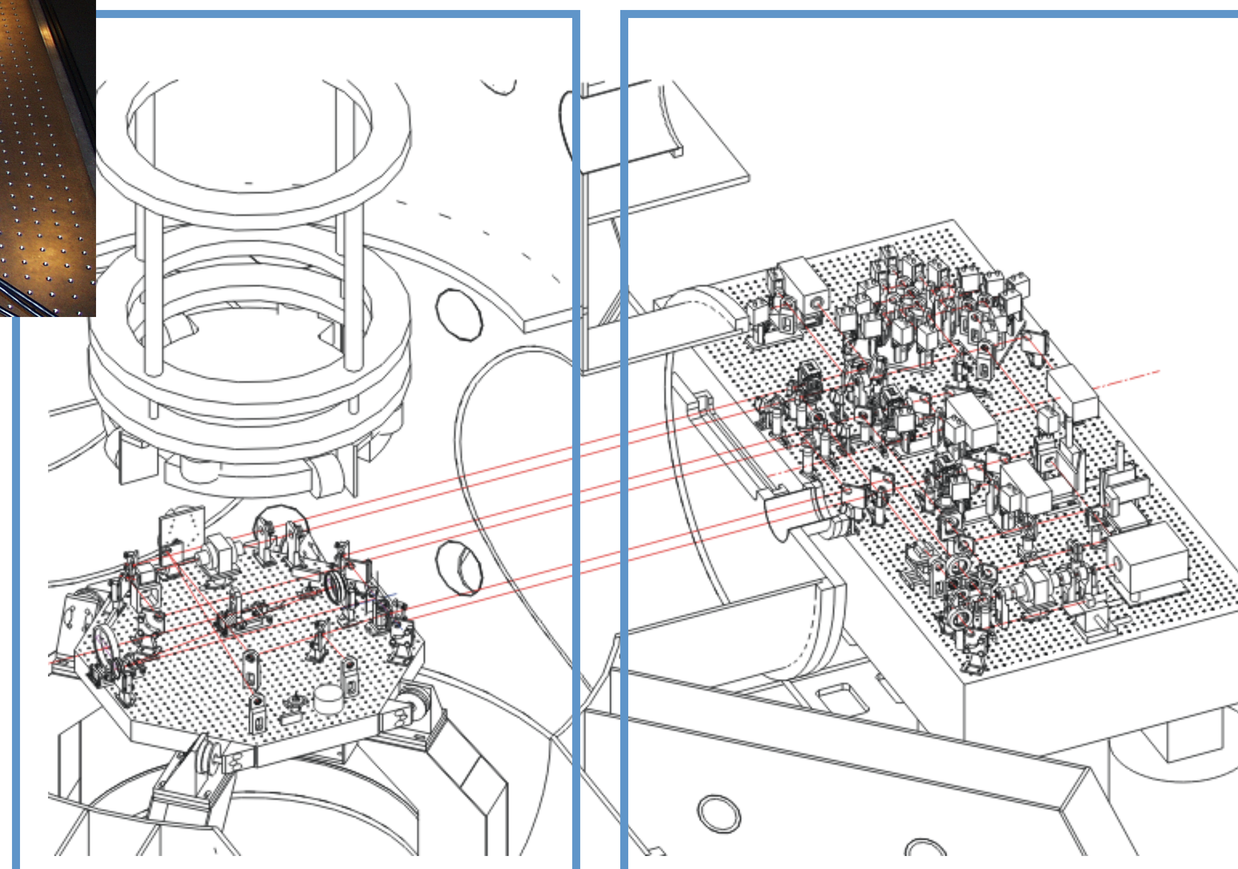

- Detection, amplification and demodulation in air on the external bench (InGaAs photodiodes array)

Detection System

- 6 benches placed in vacuum chamber
- 2 (SDB1 and SNEB) suspended and controlled
- SNEB in vacuum

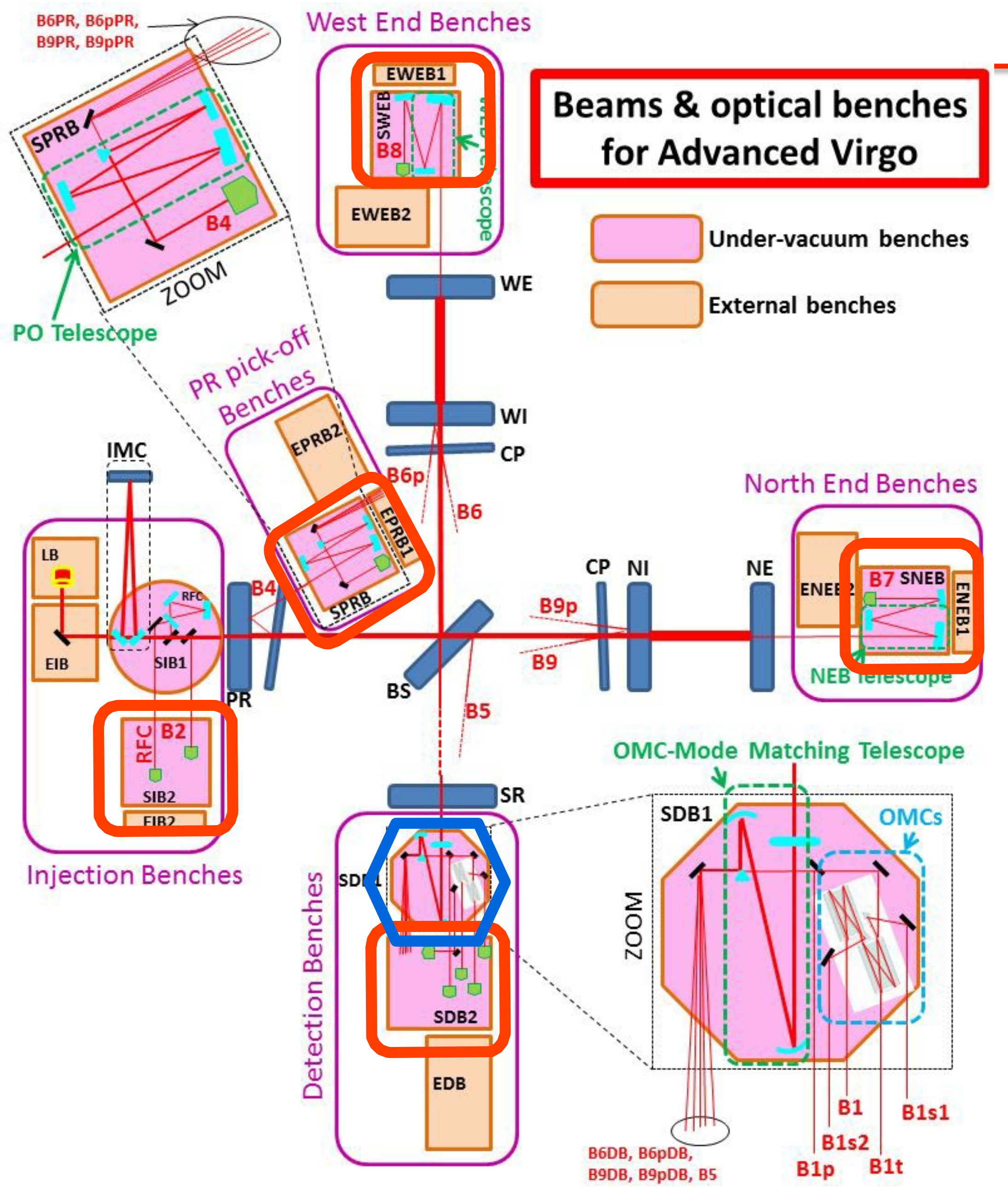

Suspended benches

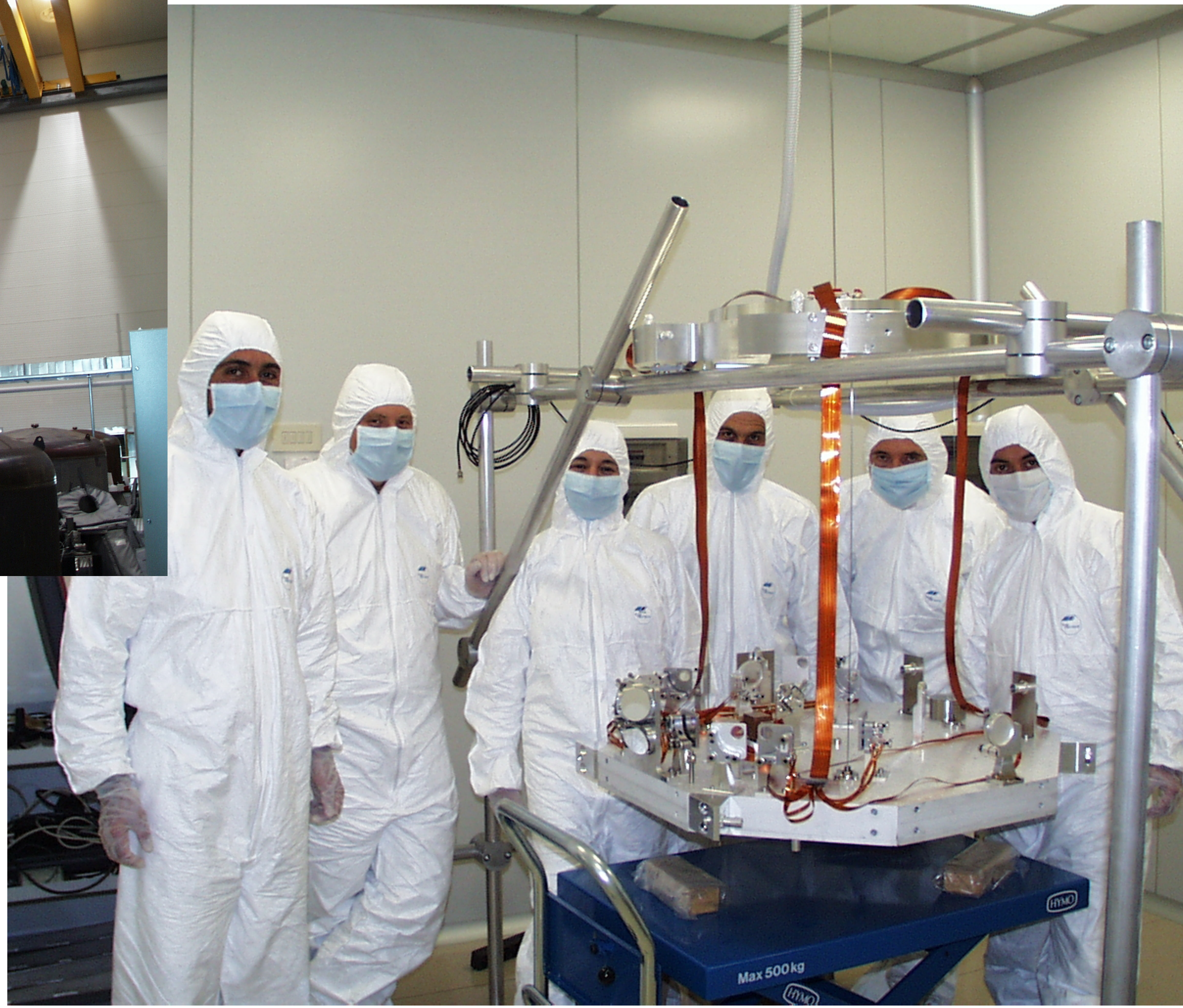

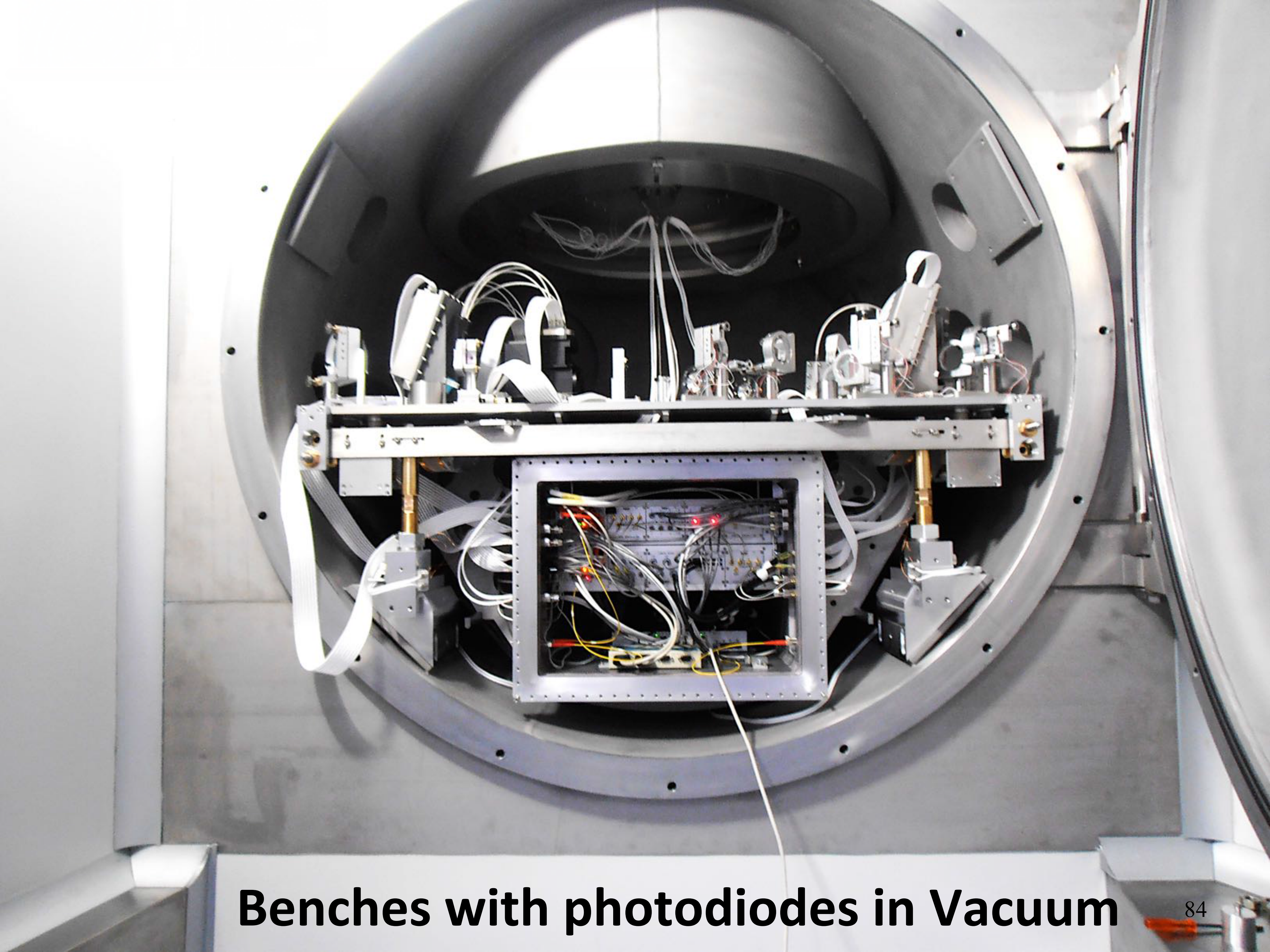

Benches with photodiodes in Vacuum

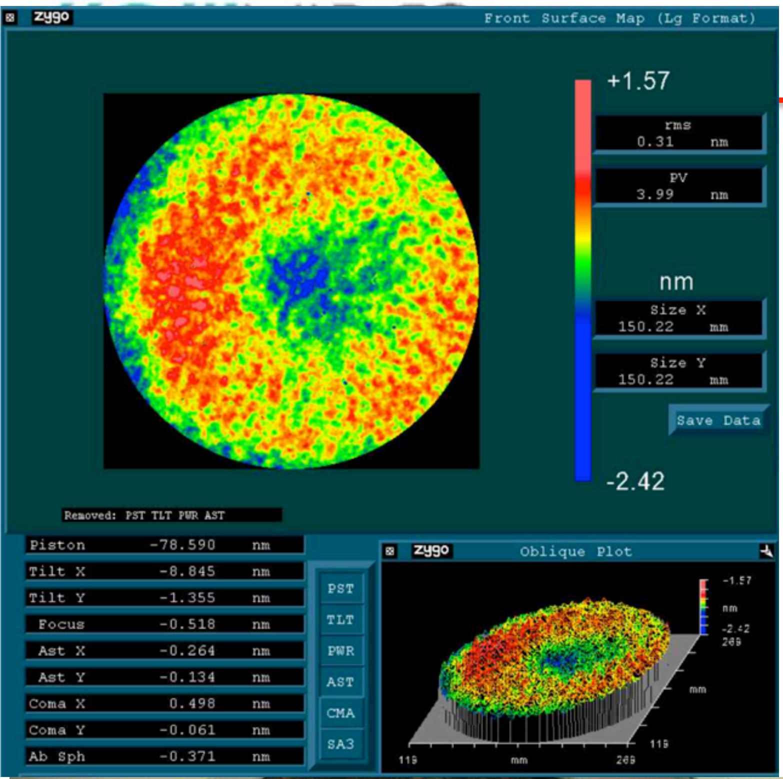

Payloads

Absorption < 0.5 ppm
Flatness O 150 cm < 0.5 nm

Test mass I ROC 1424 m
Test Mass E ROC 1690 m
Test Mass 42 kg
Diameter 350 mm
Thickness 200 mm

Beam Splitter 50%
Weight 43 kg
Diameter 500 mm
Thickness 100 mm

BS flatness O 220 cm ≤ 1 nm

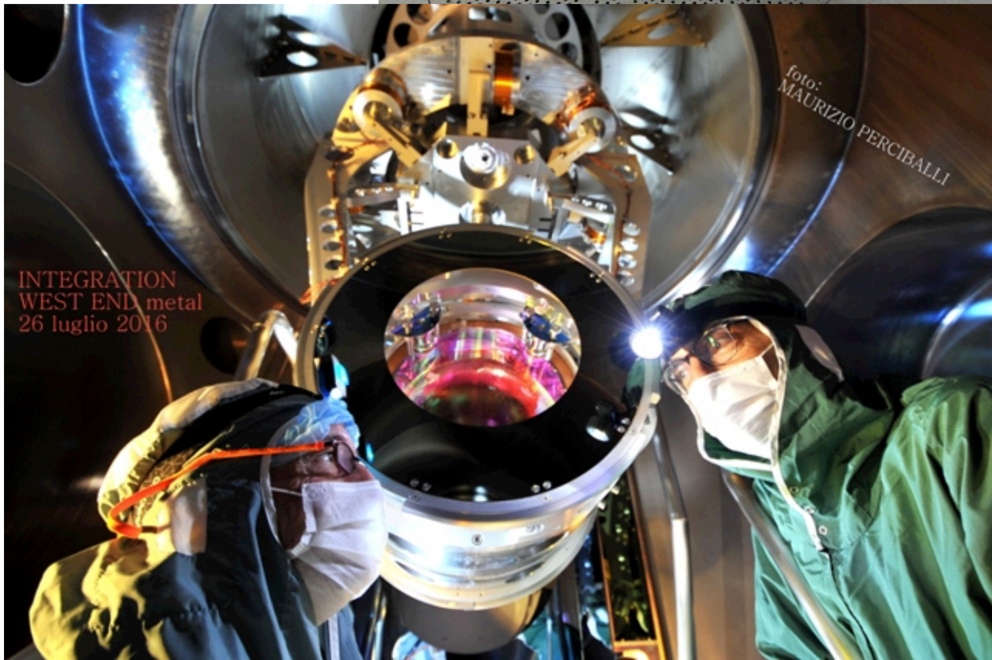

VIRGO

AdV parameters

AdV Overview, Part I		
Subsystem and Parameters	**AdV design (TDR)**	**Initial Virgo**
Sensitivity		
Binary Neutron Star Inspiral Range	134 Mpc	12 Mpc
Anticipated Max Strain Sensitivity	$3.5 \cdot 10^{-24}/\sqrt{\text{Hz}}$	$4 \cdot 10^{-23}/\sqrt{\text{Hz}}$
Instrument Topology		
Interferometer	Michelson	Michelson
Power Enhancement	Arm cavities and Power Recycling	Arm cavities and Power Recycling
Signal Enhancement	Signal Recycling	n.a.
Laser and Optical Powers		
Laser Wavelength	1064 nm	1064 nm
Optical Power at Laser Output	>175 TEM_{00} W	20 W
Optical Power at Interferometer Input	125 W	8 W
Optical Power at Test Masses	650 kW	6 kW
Optical Power on Beam Splitter	4.9 kW	0.3 kW
Test Masses		
Mirror Material	Fused Silica	Fused Silica
Main Test Mass Diameter	35 cm	35 cm
Main Test Mass Weight	42 kg	21 kg
Beam Splitter Diameter	55 cm	23 cm
Test Mass Surfaces and Coatings		
Coating Material	Ti doped Ta_2O_5	Ta_2O_5
Roughness*	< 0.1 nm	< 0.05 nm
Flatness	0.5 nm RMS	< 8 nm RMS
Losses per Surface	37.5 ppm	250 ppm (measured)
Test Mass RoC	Input Mirror: 1420 m End Mirror: 1683 m	Input Mirror: flat End Mirror: 3600 m
Beam Radius at Input Mirror	48.7 mm	21 mm
Beam Radius at End Mirror	58 mm	52.5 mm
Finesse	443	50
Thermal Compensation		
Thermal Actuators	CO_2 Lasers and Ring Heater	CO_2 Lasers
Actuation points	Compensation plates and directly on mirrors	Directly on mirrors
Sensors	Hartmann sensors and phase cameras	n.a.

AdV Overview, Part II		
Subsystem and Parameters	**AdV design (TDR)**	**Initial Virgo**
Suspension		
Seismic Isolation System	Superattenuator	Superattenuator
Degrees of Freedom of Inverted Pendulum Inertial Control	6	4
Test mass suspensions	Fused Silica Fibres (optimized geometry)	Steel Wires
Vacuum System		
Pressure	10^{-9} mbar	10^{-7} mbar
Injection System		
Input mode cleaner throughput	>96%	85% (meas.)
Detection System		
GW Signal Readout	DC-Readout	Heterodyne (RF)
Output Mode Cleaner Suppression	RF Sidebands and Higher Order Modes	Higher Order Modes
Main Photo Diode Environment	in Vacuum	in Air
Lengths		
Arm Cavity Length	3 km	3 km
Input Mode Cleaner	143.424 m	143.574 m
Power Recycling Cavity	11.952 m	12.053 m
Signal Recycling Cavity	11.952 m	n.a.
Interferometric Sensing and Control		
Lock Acquisition Strategy	Auxiliary Lasers (different wavelength)	Main Laser
Number of RF Modulations	3	1
Schnupp Asymmetry	23 cm	85 cm
Signal Recycling Parameter		
Signal Recycling Mirror Transmittance	20 %	n.a.
Signal Recycling Tuning	0.35 rad	n.a.

Conclusion

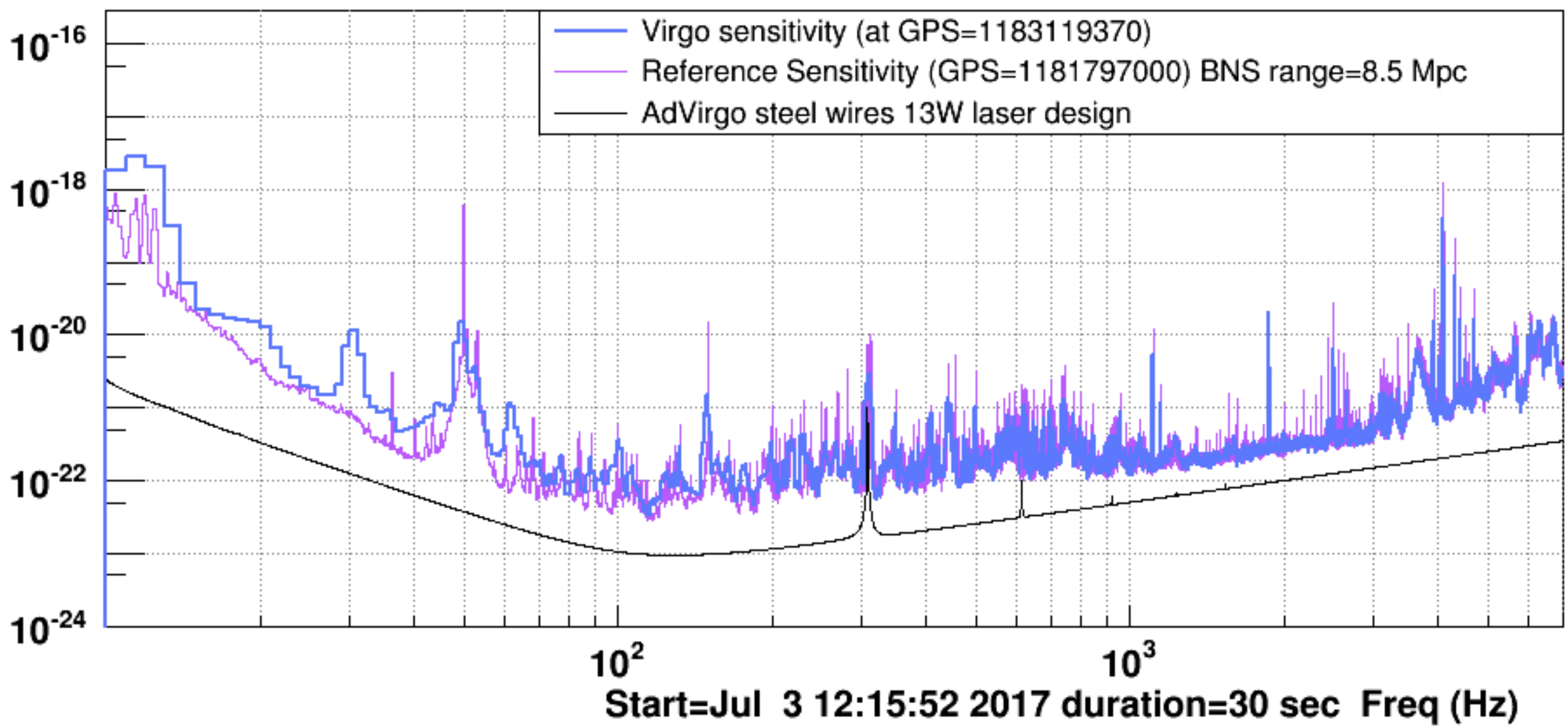

Virgo sensitivity (at GPS=1183119370)
Reference Sensitivity (GPS=1181797000) BNS range=8.5 Mpc
AdVirgo steel wires 13W laser design
10^-16
10^-18
10^-20
10^-22
10^-24
10^2
10^3
Start=Jul 3 12:15:52 2017 duration=30 sec Freq (Hz)

- EXTRA SLIDES

Lock of a single F-P cavity(II)

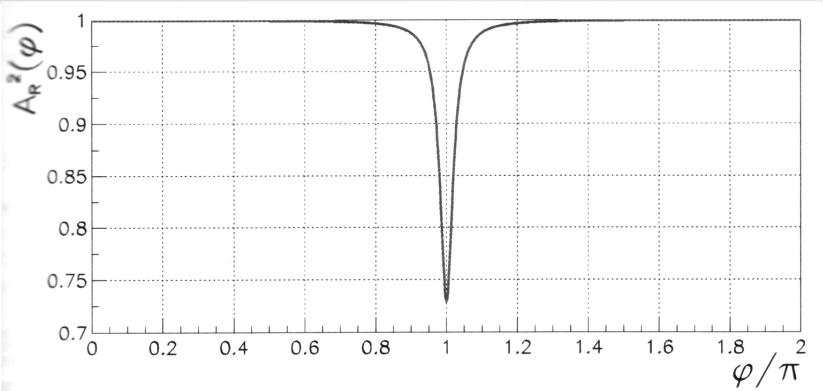

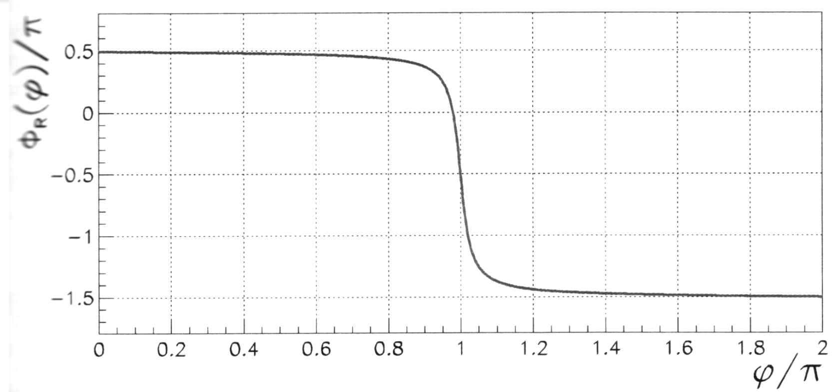

- The cavity length is such that the carrier (ω_0) is resonant

$$i\,\frac{r_1 + r_2 e^{-2ikl}}{1 + r_1 r_2 e^{-2ikl}}\,\psi_{in}$$

$$e^{-2ikl} = -1$$

-The phase of the reflected light is $\arctan(\mathrm{Im}\,\psi_r / \mathrm{Re}\,\psi_r) = \pi$ at the resonance

$$i\,\frac{r_1 - r_2}{1 - r_1 r_2}$$

At ω_0 the light reflected by the cavity has a phase shift of -180° to the respect of the incident light
and ±90° for the side-bands (for $\Omega \pm \omega_0$ far from ω_0)

$$E_r(t) = -E_0 \cdot \cos(\omega_0 t) - mE_0 \cos(\Omega t) \cdot \sin(\omega_0 t)$$

When we have a perturbation of the cavity length :

$$E_r(t) = -E_0 \cdot \cos(\omega_0 t + \phi_d) - mE_0 \cos(\Omega t) \cdot \sin(\omega_0 t + \phi_d)$$

Photo-diode output : $\left|E_r(t)\right|^2 \propto m \cdot \sin\phi_d \cos\Omega t$

The demodulated signal in phase at Ω contains the information on the length variation